

## The Characterization of Myosin–Product Complexes and of Product-Release Steps during the Magnesium Ion-Dependent Adenosine Triphosphatase Reaction

By CLIVE R. BAGSHAW and DAVID R. TRENTHAM  
*Molecular Enzymology Laboratory, Department of Biochemistry,  
University of Bristol Medical School, Bristol BS8 1TD, U.K.*

(Received 4 December 1973)

Evidence is presented that the myosin subfragment-1–ADP complex, generated by the addition of  $Mg^{2+}$  and ADP to subfragment 1, is an intermediate within the myosin  $Mg^{2+}$ -dependent adenosine triphosphatase (ATPase) turnover cycle. The existence of this species as a steady-state intermediate at pH 8 and 5°C is demonstrated by fluorescence measurements, but its concentration becomes too low to measure at 21°C. This arises because there is a marked temperature-dependence on the rate of the process controlling ADP dissociation from subfragment 1 (rate =  $1.4s^{-1}$  at 21°C,  $0.07s^{-1}$  at 5°C). In the ATPase pathway this reaction is in series with a relatively temperature-insensitive process, namely an isomerization of the subfragment-1–product complex (rate =  $0.055s^{-1}$  at 21°C,  $0.036s^{-1}$  at 5°C). By means of studies on the  $P_i$  inhibition of nucleotide-association rates, a myosin subfragment-1– $P_i$  complex was characterized with a dissociation equilibrium constant of 1.5 mM.  $P_i$  appears to bind more weakly to the myosin subfragment-1–ADP complex. The studies indicate that  $P_i$  dissociates from subfragment 1 at a rate greater than  $40s^{-1}$ , and substantiates the existence of a myosin-product isomerization before product release in the elementary processes of the  $Mg^{2+}$ -dependent ATPase. In this ATPase mechanism  $Mg^{2+}$  associates as a complex with ATP and is released as a complex with ADP. In 0.1 M-KCl at pH 8 1.0 mol of  $H^+$  is released/mol of subfragment 1 concomitant with the myosin-product isomerization or  $P_i$  dissociation, and 0.23 mol of  $H^+$  is released/mol of subfragment when ATP binds to the protein, but 0.23 mol of  $H^+$  is taken up again from the medium when ADP dissociates. Within experimental sensitivity no  $H^+$  is released into the medium in the step involving ATP cleavage.

The characterization of the intermediates associated with the  $Mg^{2+}$ -dependent ATPase\* of myosin or its proteolytic subfragments is an area of current investigation in many laboratories. In particular the properties of myosin-product complexes have been studied by a variety of techniques which have led to the conclusion that the complex formed as a result of the rapid cleavage of ATP by myosin (Lymn & Taylor, 1970) is different from that complex which can be generated by the addition of ADP and  $P_i$  to myosin. These complexes have been distinguished by spectroscopy (Morita, 1967; Seidel & Gergely, 1972; Werber *et al.*, 1972), chemical reactivity towards thiol reagents (Schaub & Watterson, 1973), and by the kinetics of their dissociation processes (Trentham *et al.*, 1972). Vinięra & Morales (1972) and Trentham *et al.* (1972) interpreted the results as evidence for an isomerization process of the myosin-product complex during the turnover of the ATPase. However, as pointed out by Seidel & Gergely (1972), the data are also compatible with a scheme involving a single-step myosin-product dissociation process, since the

complex generated by the addition of ADP to myosin may not be an intermediate within the ATPase turnover cycle. Werber *et al.* (1972) interpreted their results in this manner. According to their scheme in an assay where the initial [ATP] is greater than the initial [myosin] the myosin–ADP complex will only build up to measurable concentrations when the ATP becomes exhausted, whereas in the scheme proposed by Trentham *et al.* (1972) it is a component of the steady-state complex existing at a constant concentration during the early turnovers subsequent to the first, although under the conditions used (20°C, pH 8.0) at a concentration too low to be characterized. Following the indications of Martonosi & Malik (1972) that the dissociation rate of ADP from myosin was much decreased at low temperatures (6°C), we examined the fluorescence of the myosin steady-state complex over a range of temperatures and report evidence for the myosin–ADP complex being a genuine intermediate of the  $Mg^{2+}$ -dependent ATPase pathway.

The work described here also characterizes a  $P_i$ -binding site on subfragment 1 by rapid-reaction techniques. Analysis of  $P_i$  inhibition of the ATP association process in the transient state offers

\* Abbreviations: ATPase, adenosine triphosphatase; ATP( $\beta,\gamma$ -NH), 5'-adenylylimidodiphosphate.

considerable advantage over steady-state inhibition analysis, since the  $K_m$  of ATP for myosin is very low ( $<10^{-7}M$ ; Lymn & Taylor, 1970), compared with the dissociation constant of the myosin- $P_i$  complex. The interdependence of ADP and  $P_i$  binding is investigated by similar transient kinetic techniques. Steps in the ATPase mechanism associated with  $Mg^{2+}$  and  $H^+$  uptake and release are also characterized.

## Materials and Methods

### Proteins

Subfragment 1 was prepared from myosin extracted from rabbit skeletal muscle and characterized as described by Bagshaw & Trentham (1973). Myosin used in the  $H^+$ -release experiment was further purified by using DEAE-Sephadex A-50 (Pharmacia Fine Chemicals AB, Uppsala, Sweden) (Godfrey & Harrington, 1970).

### Nucleotides

Sodium salts of ATP and ADP were obtained from C. F. Boehringer und Soehne, Mannheim, W. Germany, and were used without further purification. ATP( $\beta,\gamma$ -NH) was prepared enzymically by a method based on that of Rodbell *et al.* (1971), scaled up 1000-fold and purified as described by Yount *et al.* (1971).

The purity of nucleotides was checked by polyethyl-eneimine-cellulose chromatography in  $0.75M-KH_2PO_4$  adjusted to pH 3.4 with HCl and analysing the chromatogram under a u.v. lamp, when nucleotide appeared as a dark spot in a fluorescent background. All the nucleotides appeared as single dark spots when 50 nmol was loaded except ADP, which contained trace amounts of material running coincident with AMP. Concentrations of adenine nucleotides were determined spectrophotometrically in a Zeiss PMQ II spectrophotometer ( $\epsilon_{259} = 15.4 \text{ mm}^{-1} \cdot \text{cm}^{-1}$  at pH 8; Bock *et al.*, 1956).

For experiments involving measurement of  $H^+$ -concentration changes ATP and ADP solutions were prepared by mixing a 10 mM nucleotide solution with 15 mM- $MgCl_2$  and adjusting the pH to pH 8.0 with aq. 0.1 M-KOH. Since ATP( $\beta,\gamma$ -NH) was prepared as the triethylamine salt, it was important to remove the triethylamine, which would act as an additional buffering component of the system. This was done by shaking the nucleotide with Dowex-50 cation-exchange resin ( $H^+$  form), centrifuging the solution and adjusting the supernatant to pH 8 with 0.1 M-KOH in the presence of 5 mM- $MgCl_2$ .

### Spectroscopic equipment

The stopped-flow spectrofluorimeter has been described elsewhere (Bagshaw *et al.*, 1972; filter 21611 should read UG11) and was used for the  $P_i$

inhibition studies. Other fluorescence experiments were carried out in a fluorimeter with manual addition of reagents. The fluorimeter was built by Dr. J. J. Holbrook. It was operated in a similar mode to that described by Holbrook (1972, Fig. 1a) with myosin subfragment 1 in cuvette 1 and a tryptophan solution in cuvette 2 to compensate for lamp intensity fluctuations. ATP was added manually from a syringe to the continuously stirred subfragment-1 solution and the fluorescence could be recorded within 5 s of addition. Dilution errors were small and could be calculated. Excitation was at 300 nm so that nucleotide absorbance of the exciting light was negligible. Emitted light was transmitted through a Wratten 18A filter. Although this system could only be used to follow reactions of half-times greater than 5 s, it offered the advantage over the stopped-flow spectrofluorimeter in being more stable for reactions in this time-range, possibly because the protein was subject to less intense u.v. light. Temperature was controlled by water circulation through the cell housing.

### Measurement of $H^+$ concentration changes

$H^+$ -concentration changes were measured by two methods depending on the time-scales involved. For times less than 5 s pH-indicator methods, essentially as outlined by Finlayson & Taylor (1969), were used with some modifications. The reactions between nucleotides and protein were monitored in the split-beam stopped-flow apparatus described by Gutfreund (1972, p. 180) with Phenol Red as the indicator ( $\epsilon_{560}$  of the anionic form =  $54 \text{ mm}^{-1} \cdot \text{cm}^{-1}$ ; Gutfreund, 1972, p. 44). The split-beam stopped-flow apparatus is particularly suitable for such measurements because the difference between the absorbance of the solutions before and after mixing is measured directly, thus increasing the base-line stability compared with a single-beam apparatus.

To calibrate the  $H^+$ -concentration changes against the absorbance change measured in the stopped-flow apparatus, reaction mixtures were made up precisely as in the stopped-flow apparatus but without the nucleotide, and the absorbance change was measured at 560 nm, when samples of standard acid or base were added to a 1 cm-light-path cuvette in the Zeiss spectrophotometer. Corrections were made for the small dilution effect on adding acid or base. The buffering capacity of  $Mg^{2+}$  complexes of nucleotide was measured independently in the region of pH 8 and in all cases was negligible in comparison with the buffering capacity of the remainder of the reaction medium.

To check whether any of the spectral changes observed resulted from indicator binding to the protein, the following control was performed. In a Perkin-Elmer 402 spectrophotometer the difference spectrum was measured in the range 400–670 nm

between 28  $\mu\text{M}$ -subfragment 1, 14  $\mu\text{M}$ -Phenol Red, 0.5M-KCl, 0.1M-Tris to keep the pH constant at pH8, and the same solution without subfragment 1. No spectral difference was observed after a small correction for light-scattering by the protein had been made. Similarly no spectral difference was observed when 4mM-ATP and 5mM-MgCl<sub>2</sub> were added to both solutions and the spectrum recorded during ATPase activity.

For longer reaction times H<sup>+</sup>-concentration changes were measured directly by using a Radiometer P 26 pH-meter linked to a Vitatron recorder. Reaction mixtures were contained in a covered thermostatically regulated vessel and stirred with a magnetic 'flea'. N<sub>2</sub> was flushed over the surface of the solution.

**Theory**

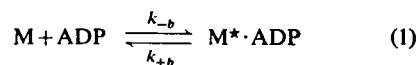
*Nomenclature*

Throughout this paper M denotes the subfragment 1 of myosin. For the *i*th step of a reaction, *k*<sub>+*i*</sub> is the forward rate constant, *k*<sub>-*i*</sub> the reverse rate constant and *K*<sub>*i*</sub> (= *k*<sub>+*i*</sub>/*k*<sub>-*i*</sub>) the equilibrium constant. *K*<sub>L</sub> denotes the dissociation equilibrium constant for the binding of the ligand L to M. [L]<sub>0</sub> and [L]<sub>∞</sub> represent the concentrations of L at zero and infinite time respectively. Starred intermediates are species with enhanced fluorescence. For the species, M\*·L, the fluorescence, F<sub>M\*·L</sub>, where this can be assigned quantitatively, is expressed relative to that of unliganded M. The fluorescence of a species is assumed to be linearly related to its concentration.

The number of intermediates that have been identified in the mechanism of the subfragment 1 Mg<sup>2+</sup>-dependent ATPase derived from rabbit skeletal myosin has increased because two states in the binding of ATP and ADP to the protein can be characterized. The evidence for this statement is presented both here and in Bagshaw *et al.* (1974), but to help cross-reference between the present and earlier work, the nomenclature for the intermediates and rate constants is correlated in Table 1.

*ADP-dissociation rate and the steady-state complex*

Equations describing the time-course of the fluorescence of myosin during single and multiple turnovers of ATP are discussed below. This provides the basis for the experiments to establish whether or not the myosin-ADP complex generated by the addition of ADP to myosin is an intermediate of the myosin ATPase pathway. Eqn. (1) defines the rate constants for formation of the complex M\*·ADP when ADP is added to M.

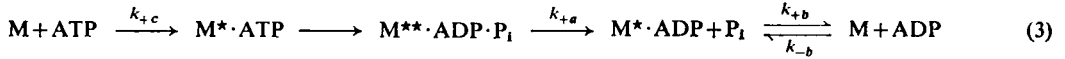
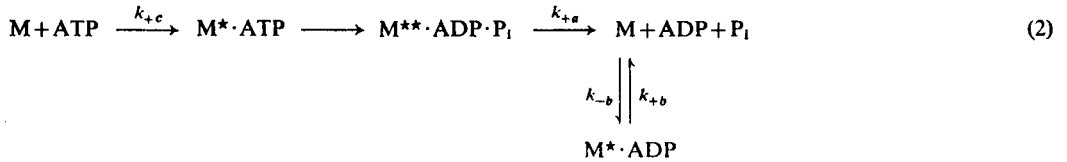


The two simplest schemes for the ATPase mechanism that illustrate the problem contain single-step binding processes and a rapid irreversible cleavage step, where the complex M\*·ADP is either formed as ATP is exhausted (eqn. 2) or as a steady-state intermediate (eqn. 3). The rate of the cleavage

Table 1. Correlation of nomenclature of intermediates and rate constants of the myosin subfragment-1 Mg<sup>2+</sup>-dependent ATPase

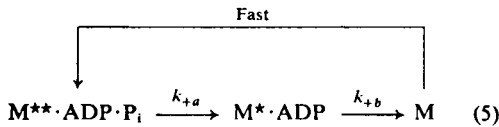
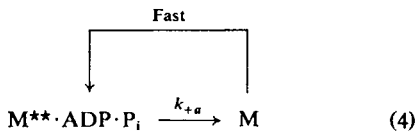
Sources of the values for the rate constants that relate to a reaction medium at 21°C of 0.1 M-KCl, 5 mM-MgCl<sub>2</sub> and 50 mM-Tris adjusted to pH8.0 with HCl are given by Bagshaw *et al.* (1974).

Eqn. (7)	Trentham <i>et al.</i> (1972)	Bagshaw <i>et al.</i> (1972)	Bagshaw & Trentham (1973)	Values
M*·ATP	E·ATP	M·ATP*	M*ATP	
M**·ADP·P <sub>1</sub>	E*·ADP·P <sub>1</sub>	M·ADP·P <sub>1</sub> *	M*ADP·P <sub>1</sub>	
M*·ADP·P <sub>1</sub>	E·ADP·P <sub>1</sub>	M·ADP·P <sub>1</sub>	MADP·P <sub>1</sub>	
M*·ADP	E·ADP	M·ADP	MADP	
<i>K</i> <sub>1</sub> <i>k</i> <sub>+2</sub>	<i>k</i> <sub>+1</sub>	<i>k</i> <sub>1</sub>	<i>k</i> <sub>+1</sub>	1.8 × 10 <sup>6</sup> M <sup>-1</sup> ·s <sup>-1</sup>
<i>k</i> <sub>-2</sub>	<i>k</i> <sub>-1</sub>	<i>k</i> <sub>-1</sub>	<i>k</i> <sub>-1</sub>	<0.02 s <sup>-1</sup>
<i>k</i> <sub>+3</sub>	<i>k</i> <sub>+2</sub>	<i>k</i> <sub>2</sub>	<i>k</i> <sub>+2</sub>	≥160 s <sup>-1</sup>
<i>K</i> <sub>3</sub>			<i>k</i> <sub>+2</sub> / <i>k</i> <sub>-2</sub>	9
<i>k</i> <sub>+4</sub>	<i>k</i> <sub>+3</sub>	<i>k</i> <sub>3</sub>	<i>k</i> <sub>+3</sub>	0.06 s <sup>-1</sup>
<i>k</i> <sub>+5</sub>	<i>k</i> <sub>+4</sub>	<i>k</i> <sub>4</sub>	<i>k</i> <sub>+4</sub>	
<i>k</i> <sub>+6</sub>	<i>k</i> <sub>+5</sub>	<i>k</i> <sub>5</sub>	<i>k</i> <sub>+5</sub>	1.4 s <sup>-1</sup>
<i>k</i> <sub>-6</sub> / <i>K</i> <sub>7</sub>		<i>k</i>		1.5 × 10 <sup>6</sup> M <sup>-1</sup> ·s <sup>-1</sup>



step,  $M^* \cdot ATP \rightarrow M^{**} \cdot ADP \cdot P_i$ , is rapid compared with  $k_{+a}$  in both schemes.

Eqns. (2) and (3) may be distinguished when multiple turnovers are examined. When excess of ATP is added to myosin the free ADP produced has little chance of recombining with M during the first few turnovers for, even though their apparent second-order binding rate constants are similar,  $[ATP] \gg [ADP]$ . Therefore the flux through the process controlled by  $k_{-b}$  is negligible, and eqns. (2) and (3) can be simplified to eqns. (4) and (5) respectively.



According to eqn. (4)  $M^{**} \cdot ADP \cdot P_i$  is the only significant component of the steady-state complex. Thus the fluorescence will remain constant after the initial rapid enhancement caused by  $M^{**} \cdot ADP \cdot P_i$  formation until the ATP is exhausted. The turnover rate will be  $k_{+a}$ .

In contrast, eqn. (5) requires  $M^* \cdot ADP$  as a component of the steady-state complex present at a significant concentration provided that  $k_{+b}$  is not very much greater than  $k_{+a}$ . The concentrations of  $M^{**} \cdot ADP \cdot P_i$  and  $M^* \cdot ADP$  in the steady-state complex are  $k_{+b}[M]_0/(k_{+a}+k_{+b})$  and  $k_{+a}[M]_0/(k_{+a}+k_{+b})$  respectively and the turnover rate is given by  $k_{+a}k_{+b}/(k_{+a}+k_{+b})$ . During the transient phase on adding excess of ATP to M,  $M^{**} \cdot ADP \cdot P_i$  reaches a maximum concentration practically equal to  $[M]_0$ . The maximum of  $M^{**} \cdot ADP \cdot P_i$  concentration is termed the initial transient state. Since  $M^* \cdot ADP$  has a different fluorescence from  $M^{**} \cdot ADP \cdot P_i$  Bagshaw *et al.*, 1972; Werber *et al.*, 1972), a difference in the fluorescence of the initial transient state compared with that of the steady state is expected. The observed fluorescence yields relative to that

of free M are defined as follows:  $F_1$ , the initial transient fluorescence;  $F_2$ , the steady-state fluorescence; and  $F_3$ , the final fluorescence when the ATP is exhausted.  $F_1 = F_{M^{**} \cdot ADP \cdot P_i}$ . At the end of the reaction when  $[ADP] \gg K_{ADP}$ ,  $M^* \cdot ADP$  is the major species present, so that  $F_3 = F_{M^* \cdot ADP}$ .  $F_2$  equals the fluorescence of the species present at their steady-state concentrations, hence:

$$F_2 = ([M^{**} \cdot ADP \cdot P_i]F_{M^{**} \cdot ADP \cdot P_i} + [M^* \cdot ADP]F_{M^* \cdot ADP})/[M]_0 = (k_{+b}F_1 + k_{+a}F_3)/(k_{+a} + k_{+b})$$

After the initial transient state and during the approach to the steady state M liberated from  $M^* \cdot ADP$  is rapidly converted back into  $M^{**} \cdot ADP \cdot P_i$ , so that

$$\frac{d[M^{**} \cdot ADP \cdot P_i]}{dt} = -k_{+a}[M^{**} \cdot ADP \cdot P_i] + k_{+b}[M^* \cdot ADP] = k_{+b}[M]_0 - (k_{+a} + k_{+b})[M^{**} \cdot ADP \cdot P_i]$$

This shows that the decay of the transient  $M^{**} \cdot ADP \cdot P_i$  concentration into its steady-state concentration is an exponential process occurring at a rate  $(k_{+a} + k_{+b})$ . The amplitude of this process  $F_1 - F_2 = k_{+a}(F_1 - F_3)/(k_{+a} + k_{+b})$ .

Analogously, when further ATP is added to the final reaction mixture, the steady-state complex is regenerated with an accompanying fluorescence change at a rate  $(k_{+a} + k_{+b})$  and an amplitude of  $F_2 - F_3 = k_{+b}(F_1 - F_3)/(k_{+a} + k_{+b})$ .

The distinctions between eqns. (2) and (3) can be summarized as follows. According to eqn. (2), when M is mixed with excess of ATP, the steady-state complex is  $M^{**} \cdot ADP \cdot P_i$  and the turnover rate is  $k_{+a}$ . According to eqn. (3) the steady-state complex is composed of  $M^{**} \cdot ADP \cdot P_i$  and  $M^* \cdot ADP$ , the turnover rate is  $k_{+a}k_{+b}/(k_{+a} + k_{+b})$  and the approach to the steady-state complex from zero time is biphasic, the rate of the slower phase being  $(k_{+a} + k_{+b})$ . Fig. 1 demonstrates these points diagrammatically.

To utilize these distinctions to the full it is important to evaluate  $k_{+a}$ . This can be done as follows. If ATP is mixed with subfragment 1 such that  $[M]_0$  is greater than  $[ATP]_0$  a single turnover of ATP hydrolysis

results which is accompanied by a change in protein fluorescence,  $F$ . When  $k_{+c}[M]_0 \gg k_{+a}$  (to ensure sufficiently rapid ATP binding), the time-course of the change in  $F$ , after the binding and cleavage steps are complete, is given by eqn. (6), where  $\alpha$ ,  $\beta$  and  $\gamma$  are defined for eqns. (2) and (3) in Table 2.

$$F = \alpha + \beta e^{-k_{+a}t} + \gamma e^{-(k_{+b} + k_{-b}[M]_0)t} \quad (6)$$

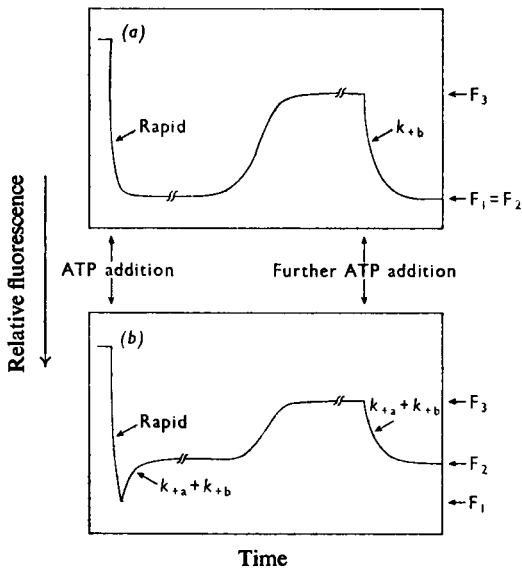


Fig. 1. Theoretical time-courses of subfragment-1 fluorescence when excess of ATP is added first to  $M$  and then to  $M^* \cdot ADP$  in (a) according to eqn. (2) and in (b) according to eqn. (3)

Rate constants of exponential processes are indicated. When  $k_{+b} \gg k_{+a}$ ,  $F_1 = F_2$  in (b) as well as (a), and so the time-courses of the fluorescence in (a) and (b) are indistinguishable. The decay in fluorescence from  $F_2$  to  $F_3$  follows a complex kinetic pattern. The onset of the decay occurs when ATP becomes exhausted or, before this, if  $\{ADP\}/K_{ADP}$  approaches the same order of magnitude as  $[ATP]/K_m$ .

$F$  is therefore characterized by two exponential phases of amplitudes  $\beta$  and  $\gamma$ . However, since  $k_{+c}[M]_0 \gg k_{+a}$  and the apparent second-order association rate constants of ATP and ADP for  $M$  are similar (i.e.  $k_{+c} \approx k_{-b}$ ; Bagshaw *et al.*, 1974),  $k_{-b}[M]_0 \gg k_{+a}$ . Reference to Table 2 shows this restraint, and the fact that  $(F_{M^{**} \cdot ADP \cdot P_i} - F_M)$  is about  $3(F_{M^* \cdot ADP} - F_M)$  (Bagshaw *et al.*, 1974) causes  $\gamma/\beta \rightarrow 0$ , and  $F$  becomes characterized by a mono-phasic exponential with a rate constant  $k_{+a}$  for either scheme (eqns. 2 or 3). Therefore a single turnover experiment does not differentiate between these schemes, but it does provide a value for  $k_{+a}$  from the observed rate of fluorescence change at saturating  $[M]_0$ .

Hence, if eqn. (3) is valid, after  $k_{+a}$  has been found from a single turnover of ATP at a high  $[M]_0$ , the value of  $k_{+b}$  should be consistent with the turnover rate and the rate and amplitude of the fluorescence change in the approach to the steady state from either decay of transient  $M^{**} \cdot ADP \cdot P_i$  or the  $M^* \cdot ADP$  displacement with ATP.

Results and Discussion

Characterization of  $M^* \cdot ADP$  as an intermediate of the  $Mg^{2+}$ -dependent ATPase

In the Theory section it was shown that eqn. (3) could be distinguished from eqn. (2) provided that  $k_{+b}$  was not much greater than  $k_{+a}$  (Fig. 1). Experiments of Martonosi & Malik (1972) suggested that the ADP dissociation rate,  $k_{+b}$ , is of the same order as the turnover rate of the  $Mg^{2+}$ -dependent ATPase at low temperatures. The time-course of the fluorescence of subfragment 1 on addition of excess of ATP was therefore studied at 5°C. When 200  $\mu M$ -ATP was added to 8  $\mu M$ -subfragment 1 at 5°C the fluorescence change leading to the steady state was biphasic (Fig. 2a). This result is qualitatively compatible with eqn. (3) but not with eqn. (2).

The protein fluorescence changes shown by Fig. 2(a) were then analysed to see if they were quantitatively consistent with eqn. (3). The maximum value of

Table 2. Coefficients  $\alpha$ ,  $\beta$  and  $\gamma$  defined by eqn. (6)

Eqn. (2) coefficients:

$$\alpha = F_M + k_{-b}(k_{+b} + k_{-b}[M]_0)^{-1}[ATP]_0(F_{M^* \cdot ADP} - F_M)$$

$$\beta = [ATP]_0[M]_0^{-1}(F_{M^{**} \cdot ADP \cdot P_i} - F_M) - k_{-b}(k_{+b} + k_{-b}[M]_0 - k_{+a})^{-1}[ATP]_0(F_{M^* \cdot ADP} - F_M)$$

$$\gamma = k_{+a}k_{-b}(k_{+b} + k_{-b}[M]_0)^{-1}(k_{+b} + k_{-b}[M]_0 - k_{+a})^{-1}[ATP]_0(F_{M^* \cdot ADP} - F_M)$$

Eqn. (3) coefficients:

$$\alpha = \alpha \text{ for eqn. (2)}$$

$$\beta = [ATP]_0[M]_0^{-1}\{(F_{M^{**} \cdot ADP \cdot P_i} - F_M) - (k_{-b}[M]_0 - k_{+a})(k_{+b} + k_{-b}[M]_0 - k_{+a})^{-1}(F_{M^* \cdot ADP} - F_M)\}$$

$$\gamma = -k_{+a}k_{+b}(k_{+b} + k_{-b}[M]_0)^{-1}(k_{+b} + k_{-b}[M]_0 - k_{+a})^{-1}[ATP]_0[M]_0^{-1}(F_{M^* \cdot ADP} - F_M)$$

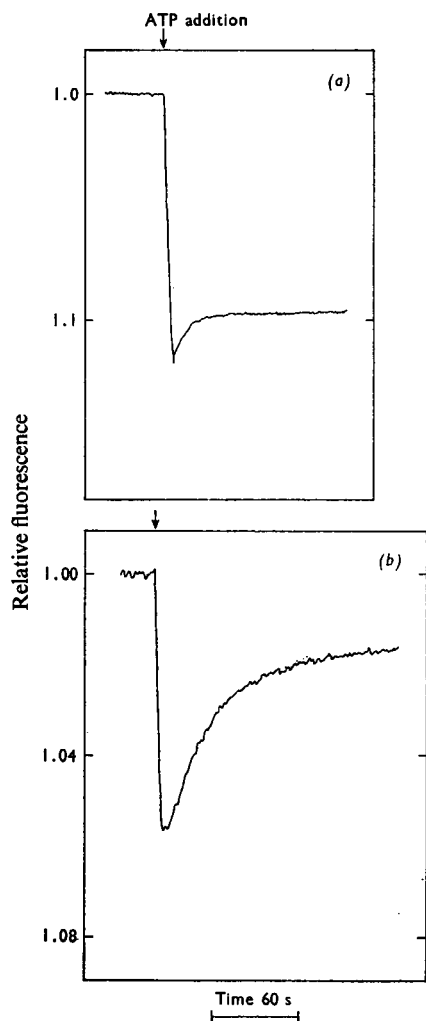


Fig. 2. Time-course of subfragment-1 fluorescence during ATP turnover at 5°C

The fluorimeter was set up as described in the Materials and Methods section. Trace (a) illustrates the time-course of the subfragment-1 fluorescence during the approach to the steady state. ATP (60  $\mu$ l) was added to 3 ml of 8  $\mu$ M-subfragment 1 to give a concentration of 200  $\mu$ M-ATP. Dilution would cause a 0.02 decrease in the fluorescence, and this correction has been applied to the fluorescence values quoted here and in the text. The rate of the process leading to the steady-state fluorescence of 1.12 was 0.136 s<sup>-1</sup>. Extrapolating this process back to 1 s gives a transient fluorescence of 1.17. The fluorescence of the steady state gradually decreased and after about 20 min reached a constant value of 1.06. Trace (b) illustrates the fluorescence change associated with a single turnover of the ATPase when 3  $\mu$ M-ATP was added to 8  $\mu$ M-subfragment 1. The rate constant of the observed exponential process was 0.036 s<sup>-1</sup>. The solvent for both traces was 0.10M-KCl-5mM-MgCl<sub>2</sub>-50mM-Tris adjusted to pH 8.0 at 21°C with HCl, so that the pH at 5°C was 8.4 when allowance is made for the heat of ionization of Tris.

the initial transient fluorescence was not recorded because of the response time of the apparatus, so  $F_1$  had to be obtained by extrapolating the observed process of Fig. 2(a) back to 1 s when the rapid binding phase would be complete. This technique gives  $F_1 = 1.17$ . Values of  $F_2$  and  $F_3$  are listed in Table 3. The observed rate of decay into the steady state in Fig. 2(a) was 0.136 s<sup>-1</sup> and, according to eqn. (3), equals  $k_{+a} + k_{+b}$ . To evaluate  $k_{+a}$ , the rate of the fluorescence change associated with a single turnover of the ATPase was examined (Fig. 2b). The observed rate of the slow phase, 0.036 s<sup>-1</sup>, equals  $k_{+a}$ , since the condition  $\gamma/\beta \rightarrow 0$  was fulfilled (see discussion of eqn. 6).  $k_{+b}$  can then be estimated from either the rate or the amplitude of the process leading to the steady-state complex as outlined in the Theory section. From the rate measurements  $k_{+b} = 0.10$  s<sup>-1</sup>. From the amplitude of the process,  $F_1 - F_2$ ,  $k_{+b} = 0.054$  s<sup>-1</sup>. Both approaches should lead to the same value for  $k_{+b}$ , but the instrument response time introduced considerable error and the results are consistent with eqn. (3). The value of  $k_{+b}$  derived from the amplitude measurement is probably more reliable.

The experiments described in Fig. 3 were carried out with a different subfragment-1 preparation from that in Fig. 2, and showed further features which were consistent with eqn. (3). The observed rate (0.14 s<sup>-1</sup>) of regeneration of the steady-state complex from  $M^* \cdot ADP$  on addition of ATP (i.e.  $F_3$  to  $F_2$ ) equalled the rate of decay of the fluorescence into the steady state (i.e.  $F_1$  to  $F_2$ ) when ATP was mixed with subfragment 1. This is required by eqn. (3), the rates of both processes being equal to  $k_{+a} + k_{+b}$ . Fig. 3 also illustrates the gradual decrease in fluorescence of the steady state owing to the build-up of  $M^* \cdot ADP$  resulting from ADP inhibition of the ATPase, as noted in the legend of Fig. 1. This effect is more apparent in Fig. 3 than in Fig. 2(a), because the initial ATP concentration was lower in Fig. 3.

At room temperature the rate of ADP dissociation from subfragment 1 is much greater than the turnover rate of the Mg<sup>2+</sup>-dependent ATPase (Bagshaw *et al.*, 1972), and so  $k_{+b} \gg k_{+a}$ . Under these conditions our experiments of the type described in Figs. 2(a) and 3 cannot distinguish between eqns. (2) and (3). However, it is useful to repeat the experiments of Fig. 2 at 21°C because it complements our other kinetic studies, which have been mostly done at room temperature (20–23°C). When 200  $\mu$ M-ATP was added to 8  $\mu$ M-subfragment 1 at 21°C, the fluorescence changes leading to the steady state occurred within the instrument response time (Fig. 4a). Values of  $F_2$  and  $F_3$  are recorded in Table 3. A single turnover experiment (Fig. 4b) was performed to evaluate  $k_{+a}$  (= 0.055 s<sup>-1</sup>). According to eqn. (3)  $k_{+a} + k_{+b}$  can be determined from the observed rate of displacement of ADP from  $M^* \cdot ADP$  by excess of ATP.

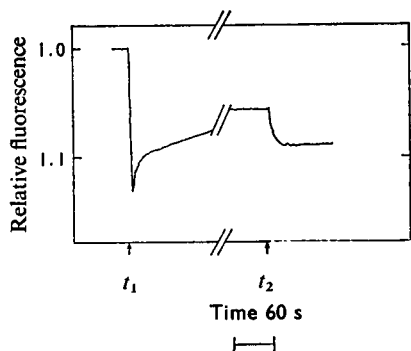


Fig. 3. Time-course of subfragment-1 fluorescence during the formation and displacement of the subfragment-1-ADP complex at 5°C

The fluorimeter was set up as described for Fig. 2 but a different subfragment-1 preparation was used. The data are used in this context to demonstrate the product inhibition and displacement of ADP. To 3 ml of 12 μM-subfragment 1, ATP was added to a concentration of 50 μM at time  $t_1$ . The form of the trace resembles Fig. 2(a), except that the steady-state fluorescence decreased more rapidly and is a consequence of the decreased [ATP] in this assay. After 600s, the interval of the break in the graph, the fluorescence reached a constant value and corresponds to  $M^* \cdot ADP$ . Addition of further ATP at time  $t_2$  to a concentration of 230 μM, regenerated the steady-state complex at a rate comparable with the initial formation of the steady-state complex ( $0.14 s^{-1}$ ). During the reproduction of this Figure base-lines of the traces were shifted to correct for dilution factors on addition of ATP and allow direct comparison of the fluorescence values. However, it should be noted the protein was subjected to u.v. light for about 15 min, possibly causing a significant drift.

At 21°C this process was too fast to measure in a manual fluorimeter, but had been measured by using a stopped-flow apparatus (Fig. 6 of Bagshaw *et al.*, 1972). The observed rate,  $1.4 s^{-1}$  ( $=k_{+a}+k_{+b}$ ), can be equated with  $k_{+b}$ , since  $k_{+a} \ll k_{+a}+k_{+b}$ .  $F_1$  was calculated by using the values for  $k_{+a}$ ,  $k_{+b}$ ,  $F_2$  and  $F_3$  (Table 3). The amplitude of the fluorescence change  $F_1-F_2$  ( $=0.005$ ) was too small to detect in the fluorescence stopped-flow apparatus in which the limit of detection was 0.01.

The experiment of Fig. 4 was repeated at 21°C but in Tris-HCl buffer at pH 8.4. The pH was then equal to that in the experiment of Fig. 2 carried out at 5°C.  $k_{+a}$  was  $0.077 s^{-1}$ , and  $k_{+a}+k_{+b}$ , and hence  $k_{+b}$ , was again too fast to measure. Therefore  $k_{+a}$  decreased by a factor of 2.1 and  $k_{+b}$  by about 20 when the temperature was lowered from 21°C to 5°C. There is an abnormally large temperature-dependence on the rate of ADP dissociation from subfragment 1, a result which agrees with Martonosi & Malik's (1972) finding with ADP and heavy meromyosin. However, our results suggest that  $K_{ADP} \leq 1 \mu M$  at both temperatures, which is smaller than the values they obtained. Our conclusion is based on the observation that the final relative fluorescence in Figs. 2(b) and 4(b) was 1.023. If the 3 μM-ADP produced in the hydrolysis of ATP had been completely bound to 8 μM-subfragment 1, the final fluorescence would have been 1.025 at 21°C and 1.023 at 5°C (based on  $F_3 = 1.067$  at 21°C and 1.06 at 5°C).

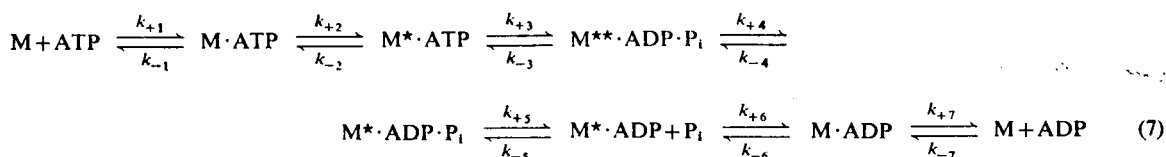
The above results show that  $M^* \cdot ADP$  is an intermediate within the ATPase turnover cycle, in accord with eqn. (3). However, eqn. (3) is an oversimplification, since the cleavage step is reversible (Bagshaw &

Table 3. Effect of temperature on subfragment-1 ATPase

$k_{+a}$ ,  $k_{+b}$ ,  $F_1$ ,  $F_2$  and  $F_3$  were evaluated on the basis of the scheme described by eqn. (3) and can be applied to eqn. (7) as indicated in the text.  $k_{+a}$  was measured as described in Figs. 2(b) and 4(b). At 5°C  $k_{+b}$  was measured from the experiment described in Fig. 2(a) and at 21°C from the rate of ADP displacement from subfragment 1 by ATP (see the text). The calculated turnover rate was derived from  $k_{+a}k_{+b}/(k_{+a}+k_{+b})$ .  $F_2$  and  $F_3$  were measured from Figs. 2(a) and 4(a). At 5°C  $F_1$  was obtained by extrapolating the observed process of Fig. 2(a) back to 1 s after mixing ATP and subfragment 1 (see the text). At 21°C  $F_1$  was calculated from  $F_2 = (k_{+b}F_1+k_{+a}F_3)/(k_{+a}+k_{+b})$ . This equation is based on schemes described by eqns. (3) and (5) as shown in the Theory section.

Temp. (°C)	$k_{+a}$ ( $s^{-1}$ )	$k_{+b}$ ( $s^{-1}$ )	Calculated turnover rate ( $s^{-1}$ )	$F_1$	$F_2$	$F_3$
5	0.036	$0.07 \pm 0.03$	$0.023 \pm 0.03$	1.17	1.12	1.06
21	0.055	1.4	0.053	1.18	1.175	1.067

Trentham, 1973). Further, stopped-flow fluorescence studies have shown that the nucleotide-binding steps are at least two-step processes, which leads to eqn. (7) representing the minimum number of intermediates of the mechanism (Bagshaw *et al.*, 1974):



The observed rate constants and fluorescence amplitudes of Figs. 2, 3 and 4 are related to more complex functions of rate constants, which are described as follows. Steps 4 and 6 are the significant rate-determining processes corresponding to steps *a* and *b* of eqn. (3). The rapid and reversible cleavage step 3 results in the equilibrium mixture  $\text{M}^* \cdot \text{ATP} + \text{M}^{**} \cdot \text{ADP} \cdot \text{P}_i$  as a component of the steady-state complex. The kinetics of the decay of this complex were reported by Bagshaw & Trentham (1973), where it was shown that the back dissociation process to free ATP was slower than the forward reaction leading eventually to free products. The flux through the process controlled by  $k_{-2}$  is therefore negligible and the rate of the decay of  $\text{M}^* \cdot \text{ATP} + \text{M}^{**} \cdot \text{ADP} \cdot \text{P}_i$  is given by  $k_{+3}k_{+4}/(k_{+3}+k_{-3})$  which corresponds to  $k_{+a}$  of the simple scheme (eqn. 3). This expression also assumes that the flux through the process controlled by  $k_{-4}$  is negligible, which is probably valid because the concentration of  $\text{M}^* \cdot \text{ADP} \cdot \text{P}_i$  remains low throughout owing to rapid  $\text{P}_i$  dissociation from  $\text{M}^* \cdot \text{ADP} \cdot \text{P}_i$  compared with the turnover rate (see below, and also Trentham *et al.*, 1972).

Since  $\text{M}^* \cdot \text{ATP}$  and  $\text{M}^{**} \cdot \text{ADP} \cdot \text{P}_i$  remain in equilibrium throughout their decay, the complex  $\text{M}^* \cdot \text{ATP} + \text{M}^{**} \cdot \text{ADP} \cdot \text{P}_i$  can be treated as having a constant fluorescence equivalent to  $F_1$ . Thus according to eqn. (7):

$$F_1 = ([\text{M}^* \cdot \text{ATP}]F_{\text{M}^* \cdot \text{ATP}} + [\text{M}^{**} \cdot \text{ADP} \cdot \text{P}_i]F_{\text{M}^{**} \cdot \text{ADP} \cdot \text{P}_i})/[\text{M}]_0 = (k_{-3}F_{\text{M}^* \cdot \text{ATP}} + k_{+3}F_{\text{M}^{**} \cdot \text{ADP} \cdot \text{P}_i})/(k_{+3} + k_{-3})$$

The dissociation rate of  $\text{M}^* \cdot \text{ADP}$  is controlled by  $k_{+6}$  (Bagshaw *et al.*, 1974) which corresponds to  $k_{+b}$  of eqn. (3). Under the conditions of a single turnover experiment when  $[\text{M}]_0 > [\text{ATP}]_0$ , the apparent

second-order association rate constant of M and ADP is  $k_{-6}/K_7$  and corresponds to  $k_{-b}$  of eqn. (3). The equations describing the time-course of protein fluorescence during single and multiple turnovers for eqn. (7) can be obtained by substitution of the

appropriate functions for  $k_{+a}$ ,  $k_{+b}$ ,  $k_{-b}$  and  $F_1$  in those equations derived for eqn. (3).

Since  $k_{+3}k_{+4}/(k_{+3}+k_{-3}) = k_{+a} = 0.055 \text{ s}^{-1}$  at 21°C, and  $K_3 = k_{+3}/k_{-3} = 9$  (Bagshaw & Trentham, 1973),  $k_{+4}$  can be calculated and equals  $0.06 \text{ s}^{-1}$ .

When the results of Table 3 are applied to eqn. (7), the composition of the steady-state complex of the subfragment-1  $\text{Mg}^{2+}$ -dependent ATPase comprises 87%  $\text{M}^{**} \cdot \text{ADP} \cdot \text{P}_i$ , 9%  $\text{M}^* \cdot \text{ATP}$  and 4%  $\text{M}^* \cdot \text{ADP}$  at 21°C and pH 8.0 and 55–64%  $\text{M}^{**} \cdot \text{ADP} \cdot \text{P}_i$ , 5–6%  $\text{M}^* \cdot \text{ATP}$  and 30–40%  $\text{M}^* \cdot \text{ADP}$  at 5°C. The distribution at 5°C assumes that the value of  $K_3$  is independent of temperature.

Schaub & Watterson (1973) demonstrated that at 25°C the steady-state complex of the myosin ATPase was protected from alkylation by *N*-ethylmaleimide, but not at 0°C. Since the myosin-ADP complex (denoted in our scheme as  $\text{M}^* \cdot \text{ADP}$ ) is susceptible to alkylation they have also postulated the change in the rate-determining step with temperature. Their technique provides independent evidence and has the advantage of being applicable to the myofibril state.

#### *P<sub>i</sub> binding*

Knowledge of the dissociation constant of  $\text{P}_i$  from  $\text{M}^* \cdot \text{ADP}$  is essential for a complete understanding of the free-energy changes during myosin and actomyosin ATPase activity. The experiments described here, which primarily characterize a  $\text{P}_i$  binding site at the active site of the ATPase in the absence of ADP, allow us to set a lower limit to the dissociation constant of  $\text{P}_i$  and  $\text{M}^* \cdot \text{ADP}$ . Addition of  $\text{P}_i$  to myosin does not itself perturb fluorescence of myosin subfragments (Werber *et al.*, 1972); therefore if  $\text{M} \cdot \text{P}_i$  exists, the kinetics of its formation and decay cannot be studied directly by the fluorescence stopped-flow technique. Trentham *et al.* (1972) reported that



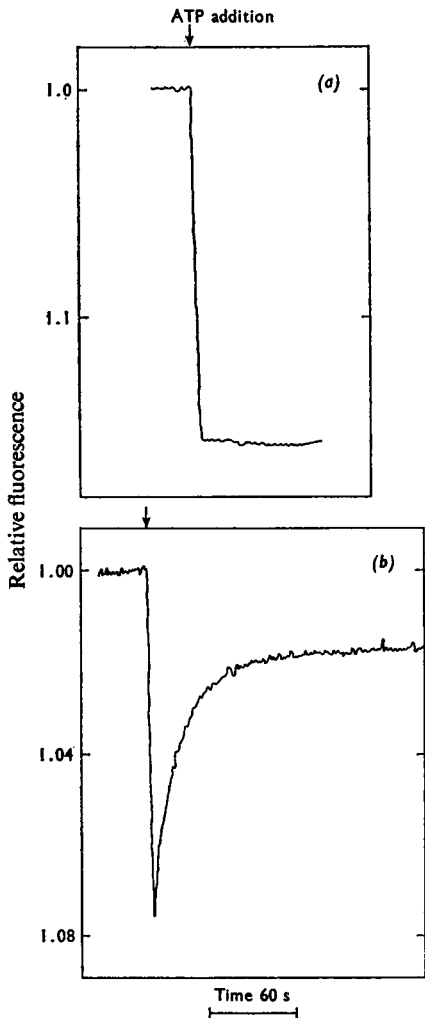


Fig. 4. Time-course of subfragment-1 fluorescence during ATP turnover at 21°C

The experiment was repeated under conditions identical with those in Fig. 2, but at 21°C and pH 8.0. Trace (a), corresponding to trace (a) of Fig. 2, remained at a constant fluorescence of 1.175 until the ATP was exhausted, when the value fell to 1.067. The time-course of the trace was similar to that of the difference absorption spectrum noted by Morita (Fig. 6, 1967) and that reported by Mandelkow & Mandelkow (Fig. 1, 1973). The time taken from addition of ATP to the point where the fluorescence enhancement fell to half-maximal was 420s, indicating a steady-state ATPase rate of  $0.06s^{-1}$  (Morita, 1967). Trace (a) provides a measure of the response time of the instrument, since the fluorescence-enhancement process is known to occur at a rate of  $150s^{-1}$  under these conditions (Bagshaw *et al.*, 1974). A stable reading was obtained after 5s. Trace (b) corresponds to trace (b) of Fig. 2. The rate constant of the observed exponential process was  $0.055s^{-1}$ . Although eqn. (3) demands this rate to be independent of [subfragment 1], at high [subfragment 1] a 25% increase in rate was noted on doubling the [subfragment 1]. This increment, however, is within the experimental error.

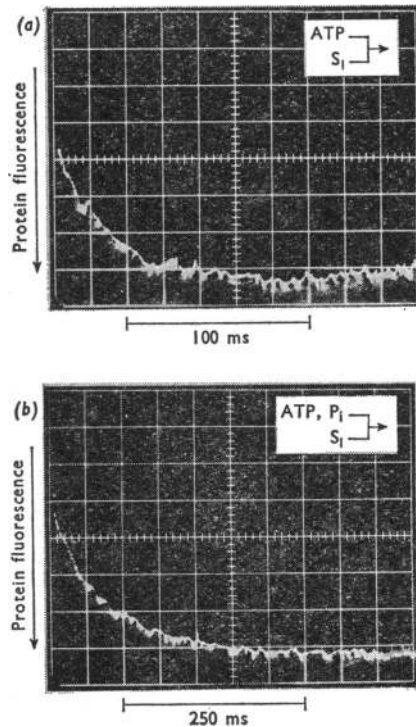


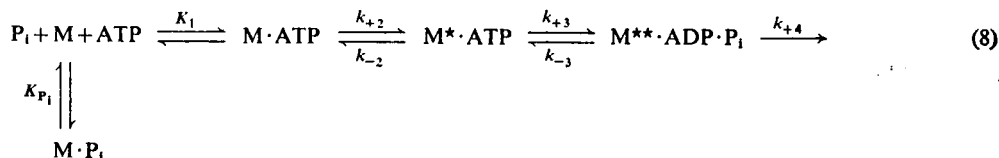
Fig. 5. Stopped-flow spectrophotometric record of the protein fluorescence during a reaction of ATP with subfragment 1 in the presence of  $P_i$

Both syringes contained 0.10M-KCl-5mM-MgCl<sub>2</sub>-50mM-Tris adjusted to pH 8.0 with HCl. In trace (a) one syringe contained 3  $\mu$ M-subfragment 1 ( $S_1$ ) and the other 26  $\mu$ M-ATP. In trace (b) the second syringe contained 26  $\mu$ M-ATP and 5mM-KH<sub>2</sub>PO<sub>4</sub> adjusted to pH 8.0 with KOH (reaction-chamber concentrations).  $k_{obs.}$  was obtained from a logarithmic plot of the traces and for (a) was  $31s^{-1}$  and for (b) was  $12s^{-1}$ .

1 mM- $P_i$  had no effect on the turnover rate of the heavy meromyosin  $Mg^{2+}$ -dependent ATPase in the presence of 50  $\mu$ M-ATP. Under similar conditions with subfragment 1 we show here that the amplitude of the fluorescence of the steady-state complex at room temperature is unaltered by the addition of up to 10mM- $P_i$ . Both these observations suggest the dissociation equilibrium constant  $K_P$  for the  $M \cdot P_i$  complex is several orders of magnitude greater than the  $K_m$  of myosin for ATP. Analysis of  $P_i$  binding to M by transient kinetic methods is more sensitive than by the steady-state approach. This is because, in the presence of  $P_i$ , subfragment 1 will consist of a mixture of M and  $M \cdot P_i$ , and the rate of formation of the steady-state complex at relatively low [ATP]

will be decreased by a factor  $1 + ([M \cdot P_i]/[M])$ . The rate of formation of the steady-state complex can be monitored by using the stopped-flow spectrofluorimeter even though the small  $K_m$  of ATP means that the steady-state rate of the ATPase may hardly be affected at all.

By using the stopped-flow technique it was shown that  $P_i$  in the 1–10 mM concentration range inhibited the association rate of ATP to subfragment 1 although the amplitude of the fluorescence change (within  $\pm 20\%$   $\Delta F$ ) was not affected (Fig. 5). The observed rate of ATP binding to subfragment 1 in the presence of  $P_i$  was the same whether  $P_i$  was preincubated with the ATP or the subfragment 1 (at least up to rates of  $40 s^{-1}$ , the upper limit studied). These results are consistent with a mechanism in which  $P_i$  binds rapidly but weakly at the active site of myosin subfragment 1 as described by eqn. (8):



Where  $K_1 = [M \cdot ATP]/[M][ATP]$  and  $K_{P_i} = [M][P_i]/[M \cdot P_i]$  and refer to rapid equilibria. When ATP and  $P_i$  are mixed with M in the fluorescence stopped-flow apparatus the generation of  $M^* \cdot ATP$  and  $M^{**} \cdot ADP \cdot P_i$  is observed. Small values of  $k_{-2}$  and  $k_{+4}$  allow the flux through the processes controlled by  $k_{-2}$  and  $k_{+4}$  to be ignored in the treatment of the kinetic analysis of eqn. (8). Conditions in which this is justified are presented below. From the conservation of myosin sites:

$$[M] = \frac{[M]_0 - ([M^* \cdot ATP] + [M^{**} \cdot ADP \cdot P_i])}{1 + K_1[ATP] + ([P_i]/K_{P_i})}$$

When  $[ATP]_0 \gg [M]_0$

$$\begin{aligned}
 d([M^* \cdot ATP] + [M^{**} \cdot ADP \cdot P_i])/dt &= \\
 k_{+2}[M \cdot ATP] &= k_{+2}K_1[M][ATP] = \\
 k_{+2}\{[M]_0 - ([M^* \cdot ATP] + [M^{**} \cdot ADP \cdot P_i])\} & \\
 1 + (1/K_1[ATP]) + ([P_i]/K_{P_i}[ATP]) &
 \end{aligned}$$

so that  $([M^* \cdot ATP] + [M^{**} \cdot ADP \cdot P_i])$  changes exponentially with time. The observed change of fluorescence is proportional to  $([M^* \cdot ATP] + [M^{**} \cdot ADP \cdot P_i])$  and hence the rate of this exponential process,  $k_{obs.}$ , is related to  $[P_i]$  as follows:

$$k_{obs.}^{-1} = \frac{1 + (1/K_1[ATP])}{k_{+2}} + \frac{[P_i]}{k_{+2}K_1K_{P_i}[ATP]} \quad (9)$$

Therefore a plot of  $k_{obs.}^{-1}$  against  $[P_i]$  at fixed  $[ATP]$  yields a series of lines intersecting at  $[P_i] = -K_{P_i}$  with gradients proportional to  $[ATP]^{-1}$ . Experiments as exemplified by Fig. 5 were carried out over a range of ATP and  $P_i$  concentrations and the data were plotted according to eqn. (9) in Fig. 6(a). From these results it was concluded that  $P_i$  binds to myosin subfragment 1 competitively with ATP with a dissociation constant  $K_{P_i} = 1.5$  mM at pH 8.0 and 20°C. Fig. 6(b) shows the secondary plot of the gradients against  $[ATP]^{-1}$ , from which the slope  $(=1/k_{+2}K_1K_{P_i})$  is  $3.8 \times 10^{-4} s$ . This gives  $k_{+2}K_1 = 1.75 \times 10^6 M^{-1} \cdot s^{-1}$ , and corresponds to the apparent association rate of ATP to subfragment 1. Since a monophasic process with the same  $k_{obs.}$  was obtained when  $P_i$  was premixed with the subfragment 1 instead of ATP, for  $k_{obs.}$  up to  $40 s^{-1}$ ,  $P_i$  must dissociate from  $M \cdot P_i$  with a rate constant exceeding  $40 s^{-1}$ .

A more rigorous treatment of eqn. (8) yields an integrated rate expression for the production of  $M^* \cdot ATP$  and  $M^{**} \cdot ADP \cdot P_i$  as follows:

$$[M^* \cdot ATP] + [M^{**} \cdot ADP \cdot P_i] = \frac{[M]_0}{k_x(k_x + k_y)} (1 - e^{-(k_x + k_y)t}) \quad (10)$$

where

$$k_x = \frac{k_{+2}}{1 + (1/K_1[ATP]) + ([P_i]/K_{P_i}[ATP])}$$

and

$$k_y = \frac{(k_{-2}k_{-3} + k_{+3}k_{+4})}{(k_{+3} + k_{-3})}$$

The simplification introduced for the first treatment of eqn. (8) was that  $k_x \gg k_y$ , and hence  $k_{obs.} \rightarrow k_x$ . This is valid for the concentrations of ATP and  $P_i$  used here, since the observed rates are in excess of  $3 s^{-1}$ , whereas  $k_y = 0.055 s^{-1}$  (Bagshaw *et al.*, 1974). This situation is also reflected in the amplitude of the observed fluorescence change. Setting  $t = \infty$  in eqn. (10) (i.e. when the steady state is attained) shows the final concentration of  $M^* \cdot ATP + M^{**} \cdot ADP \cdot P_i = [M]_0$  regardless of  $[P_i]$  if  $k_x \gg k_y$ . Eqn. (10) is presented, since the approximation leading to

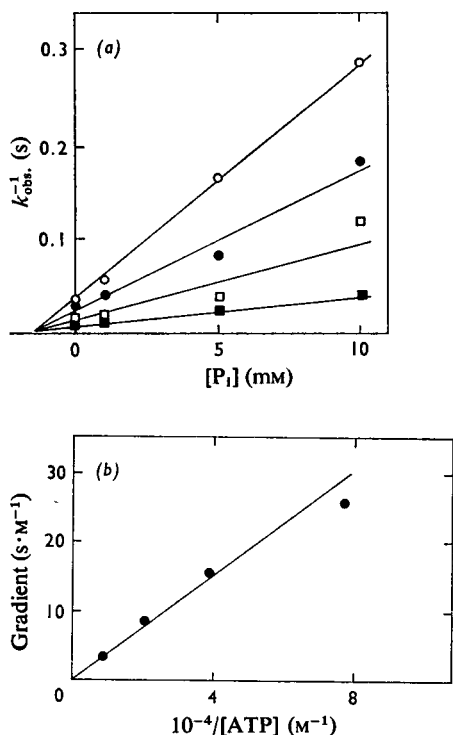


Fig. 6. Plot of  $P_1$  inhibition data to determine  $K_{P_1}$ .

Experiments as exemplified in Fig. 5 were carried out over a range of ATP ( $\circ$ , 13  $\mu\text{M}$ ;  $\bullet$ , 26  $\mu\text{M}$ ;  $\square$ , 52  $\mu\text{M}$ ;  $\blacksquare$ , 104  $\mu\text{M}$ ) and  $P_1$  concentrations. In (a) the data were plotted according to eqn. (9) from which  $K_{P_1} = 1.5 \text{ mM}$  at pH 8.0 and 21°C. In (b) the gradients of the lines in (a) were plotted against  $[\text{ATP}]^{-1}$  and the gradient of the resulting line was  $3.8 \times 10^{-4} \text{ s} (= 1/k_{+2} K_1 K_{P_1}$  according to eqn. 9).

eqn. (9) is not justified when  $k_y$ , the effective dissociation rate of the high-fluorescence species, is in the same order, as  $k_{\text{obs}}$ , as might arise with ATP analogues or assays where the  $[P_1]/[\text{ATP}]$  ratio is greater than those investigated here.

In our studies on the inhibition of the ATP-association rate the  $P_1$  concentration was restricted to a maximum of 20 mM.  $P_1$  did not cause inhibition of  $\text{Mg} \cdot \text{ATP}$  binding by lowering the effective free  $\text{Mg}^{2+}$  concentration since similar stopped-flow traces were obtained for ATP binding to subfragment 1 at a constant 5 mM- $P_1$ , and  $\text{Mg}^{2+}$  varied between 5 and 20 mM. The ionic-strength changes arising from changes in  $[P_1]$  in the experiment described by Fig. 6 would have an insignificant effect on the ATP association rate (Bagshaw *et al.*, 1974). The use of a technique involving competition with the ATP molecule that is hydrolysed indicates that we are here analysing  $P_1$  binding at the catalytic site.

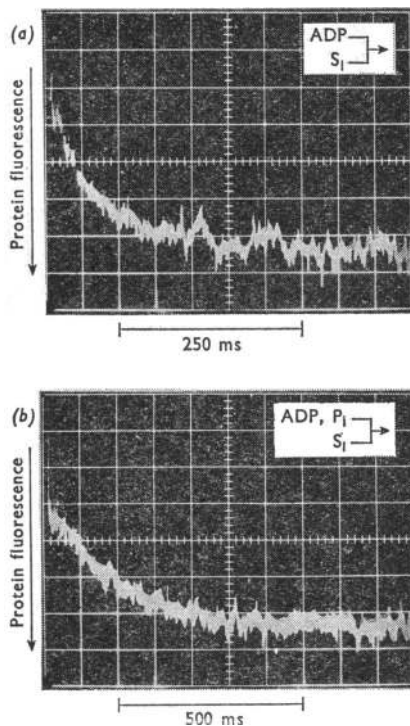


Fig. 7. Stopped-flow spectrophotometric record of the protein fluorescence during the reaction of ADP with subfragment 1 in the presence of  $P_1$ .

Both syringes contained 0.10 M-KCl-5 mM- $\text{MgCl}_2$ -50 mM-Tris adjusted to pH 8.0 with HCl. In trace (a) one syringe contained 4.9  $\mu\text{M}$ -subfragment 1 ( $S_1$ ) and the other 48  $\mu\text{M}$ -ADP. In trace (b) the second syringe also contained 5 mM- $\text{KH}_2\text{PO}_4$  adjusted to pH 8.0 with KOH (reaction-chamber concentrations). From logarithmic plots of the traces  $k_{\text{obs}}$ , for (a) was  $12 \text{ s}^{-1}$  and for (b) was  $4.7 \text{ s}^{-1}$ .

Secondary  $P_1$ -binding sites on the light meromyosin fragment of myosin have been reported by Harrington & Himmelfarb (1972) and control the polymerization state of the myosin molecule.

It is important to determine the significance of the  $\text{M} \cdot P_1$  complex, with respect to the elementary processes of the ATPase. To establish the relationship between  $K_{P_1}$  and the equilibrium constant  $k_{+5}/k_{-5}$  of eqn. (7), experiments were carried out to determine the interdependence of ADP and  $P_1$  binding to subfragment 1. Results have been presented above which show that ADP can bind to subfragment 1 in the absence of  $P_1$ , and  $P_1$  can bind to subfragment 1 in the absence of ADP, which could be taken as evidence for a random mechanism of product dissociation. If ADP and  $P_1$  binding were completely independent,  $P_1$  would not affect the association or

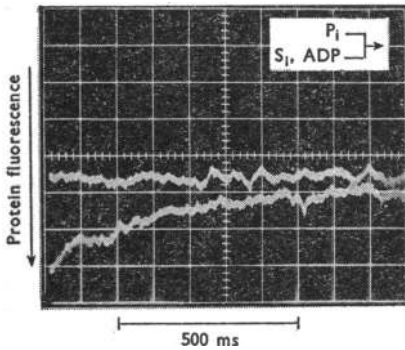


Fig. 8. Stopped-flow spectrophotometric record of protein fluorescence when subfragment 1 in the presence of ADP is mixed with  $P_i$ .

One syringe contained  $6.4\mu\text{M}$ -subfragment 1 ( $S_1$ ) and  $20\mu\text{M}$ -ADP and the other  $10\text{mM}$ - $\text{KH}_2\text{PO}_4$  adjusted to pH 8.0 with KOH (reaction-chamber concentrations). Both syringes contained  $0.10\text{M}$ -KCl- $5\text{mM}$ - $\text{MgCl}_2$ - $50\text{mM}$ -Tris adjusted to pH 8.0 with HCl. The horizontal trace was obtained by triggering the oscilloscope several seconds after mixing. The scale of the fluorescence amplitude is amplified approximately twofold compared with Fig. 7, and the observed fluorescence change is about 3%.

dissociation rate of ADP and myosin. However, in attempting to generate  $\text{M}^*\cdot\text{ADP}\cdot\text{P}_i$  by addition of ADP and  $\text{P}_i$  to subfragment 1 results were obtained which indicated  $\text{P}_i$  does not readily bind to  $\text{M}^*\cdot\text{ADP}$  although it may bind to  $\text{M}\cdot\text{ADP}$ .

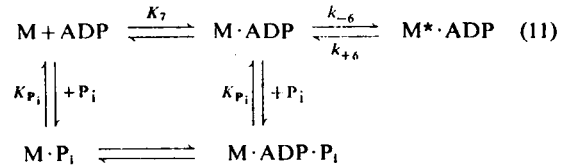
First the rate and amplitude of subfragment-1 fluorescence enhancement when the protein was mixed with ADP were reduced in the presence of  $\text{P}_i$ . This result is shown in Fig. 7.

Secondly when excess of ATP was added to a mixture of subfragment 1, saturated with ADP (i.e. concentration  $>K_{\text{ADP}}$ ) and  $\text{P}_i$  (concentration  $>K_{\text{P}_i}$ ), a biphasic increase in the fluorescence was obtained. The observed rates were consistent with a rapid displacement of  $\text{P}_i$  [ $k_{\text{obs}}$ , described by eqn. (9)] followed by a slow phase corresponding to the displacement of ADP at  $1.4\text{s}^{-1}$  (see Fig. 6 of Bagshaw *et al.*, 1972). The amplitudes of the phases were dependent on the relative concentrations of ADP and  $\text{P}_i$  and were of comparable magnitude when  $[\text{ADP}]/K_{\text{ADP}} = [\text{P}_i]/K_{\text{P}_i}$ .

Finally when high concentrations of  $\text{P}_i$  were added to  $\text{M}^*\cdot\text{ADP}$ , generated by the addition of ADP to subfragment 1, a reduction in fluorescence enhancement was noted whose rate and amplitude were consistent with the partial decay of  $\text{M}^*\cdot\text{ADP}$  to low-fluorescence forms of myosin (e.g.  $\text{M}\cdot\text{P}_i$ ). Fig. 8 shows that addition of  $10\text{mM}$ - $\text{P}_i$  to subfragment 1 in

the presence of  $20\mu\text{M}$ -ADP results in a decrease in fluorescence of about 40% that associated with complete displacement of ADP from  $\text{M}^*\cdot\text{ADP}$  and at a rate of  $3.7\text{s}^{-1}$ .

Qualitatively it can be seen  $\text{P}_i$  must bind preferentially to the low fluorescence forms of myosin compared with  $\text{M}^*\cdot\text{ADP}$ . One scheme which describes this is given by eqn. (11):



where  $K_7 = k_{+7}/k_{-7} = [\text{M}][\text{ADP}]/[\text{M}\cdot\text{ADP}]$ ,  $K'_{\text{P}_i} = [\text{M}\cdot\text{ADP}][\text{P}_i]/[\text{M}\cdot\text{ADP}\cdot\text{P}_i]$

This scheme can be analysed quantitatively by measuring the rates of subfragment-1 fluorescence enhancement by ADP in the presence of  $\text{P}_i$  as described in Fig. 7. The expression describing the fluorescence enhancement of subfragment 1 (i.e.  $\text{M}^*\cdot\text{ADP}$  production) when  $[\text{ADP}]_0 \gg [\text{M}]_0$  is similar to eqn. (10), but with an additional term describing  $\text{P}_i$  binding to  $\text{M}\cdot\text{ADP}$ .

$$[\text{M}^*\cdot\text{ADP}] = k'_x(k'_x + k'_y)^{-1}[\text{M}]_0(1 - e^{-(k'_x + k'_y)t}) \quad (12)$$

where

$$k'_x = \frac{k_{-6}}{1 + (K_7/[\text{ADP}]) + ([\text{P}_i]/K'_{\text{P}_i}) + (K_7[\text{P}_i]/K_{\text{P}_i}[\text{ADP}])}$$

and

$$k'_y = k_{+6}$$

The dissociation rate of ADP from  $\text{M}^*\cdot\text{ADP}$  is controlled by  $k_{+6}$ , which equals  $1.4\text{s}^{-1}$  under these conditions (Bagshaw *et al.*, 1972) and is therefore an order of magnitude greater than the equivalent function  $k_y$  of eqn. (10) for the ATP scheme (eqn. 8). Consequently at the low ADP concentrations used here  $k_{+6}$  significantly contributes to the observed rate of the fluorescence change,  $k_{\text{obs}}$ , when ADP binds to M in the presence of  $\text{P}_i$ . From the exponent of eqn. (12) an expression is obtained for the dependence of  $k'_{\text{obs}}$  on  $[\text{P}_i]$  allowing for  $k_{+6}$  as follows:

$$\begin{aligned} (k'_{\text{obs}} - k_{+6})^{-1} &= \frac{1 + (K_7/[\text{ADP}])}{k_{-6}} + \\ &\left( \frac{1}{K'_{\text{P}_i}k_{-6}} + \frac{K_7}{K_{\text{P}_i}k_{-6}[\text{ADP}]} \right) [\text{P}_i] \quad (13) \end{aligned}$$

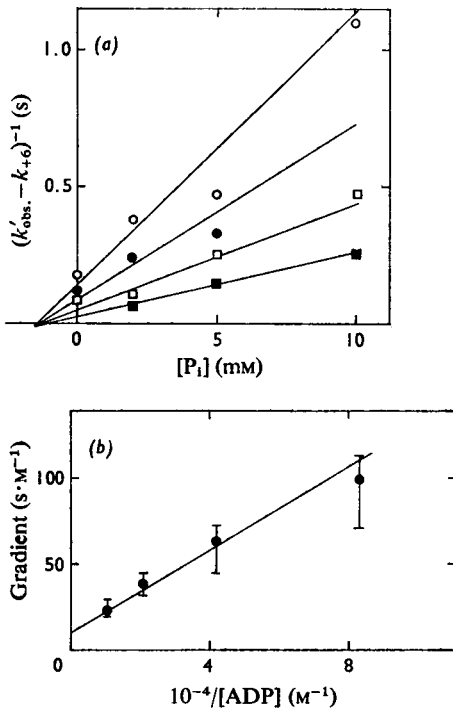


Fig. 9. Inhibition of ADP binding by  $P_i$

Experiments as exemplified in Fig. 7 were carried out over a range of ADP ( $\circ$ ,  $12 \mu\text{M}$ ;  $\bullet$ ,  $24 \mu\text{M}$ ;  $\square$ ,  $48 \mu\text{M}$ ;  $\blacksquare$ ,  $96 \mu\text{M}$ ) and  $P_i$  concentrations. In (a) the data were plotted according to eqn. (13) from which the solid lines, fitted by the reiterative procedure described below, give a value of  $K_{P_1} = 1.5 \text{ mM}$ . In (b) the value of the ordinate intercept and  $k_{-6}$  gives an estimate of  $K'_{P_1} = 0.5 \text{ mM}$ . The procedure adopted to evaluate the data was as follows. First, the gradients of each series of data points in (a) were estimated to fall within the error bars of (b). The ordinate intercept in (b),  $= 1/K'_{P_1}k_{-6}$ , is therefore significant and allows boundary values to be placed on  $K'_{P_1}$  of  $0.24\text{--}1.0 \text{ mM}$ . Knowing  $K_{P_1}$  from the ATP to be  $1.5 \text{ mM}$ , allows the coordinates of the point of intersection in (a) to be evaluated more precisely since these are defined by an abscissa value of  $-K_{P_1}$  and an ordinate value of  $(K_{P_1} - K'_{P_1})/(K'_{P_1}k_{-6})$ . Fixing this point allows the lines in (a) to be drawn, from which the values of the gradients were obtained and plotted in (b). The value of  $k_{+6}$  was taken to be  $1.4 \text{ s}^{-1}$  (Bagshaw *et al.*, 1972).  $k_{-6}$  was estimated to be  $200 \text{ s}^{-1}$  for this preparation of subfragment 1 from the rate of fluorescence change when the protein was mixed with high concentrations of ADP (Bagshaw *et al.*, 1974).

slope of  $K_7/(K'_{P_1}k_{-6})$ . When the ADP data from experiments exemplified by Fig. 7 are plotted according to eqn. (13) as in Fig. 9(a) the point of intersection ( $-K_{P_1}$ ) lies between  $-1$  and  $-2 \text{ mM}$  on the abscissa and agrees with the value of  $K_{P_1}$  obtained from the ATP data. Although the ordinate value cannot be accurately determined from this plot it is clear that  $K'_{P_1}$  cannot be very much smaller than  $K_{P_1}$  otherwise the intersection would lie far below the abscissa (the extreme model where  $P_i$  only binds to  $M \cdot \text{ADP}$  results in a series of parallel lines at each ADP concentration). The value of  $K'_{P_1}$  can be found from the intercept of the plot of the gradient of the lines in Fig. 9(a) against  $[\text{ADP}]^{-1}$  as in Fig. 9(b). The best fit for both graphs was found by a reiterative procedure. Although the data are scattered, there is a positive ordinate intercept in Fig. 9(b) and therefore  $P_i$  binds to  $M \cdot \text{ADP}$ . The lines drawn in Fig. 9(a) and (b) give  $K_{P_1} = 1.5 \text{ mM}$  and  $K'_{P_1} = 0.5 \text{ mM}$ . The experimental error was relatively large in the ADP data since the fluorescence enhancement of subfragment 1 induced by ADP is only one-third of that induced by ATP, and this is further decreased in the presence of  $P_i$ . The amplitudes of the fluorescence change were consistent with eqn. (12) and progressively decreased with increasing  $[P_i]$ . For  $10 \mu\text{M}$ -ADP the amplitude was reduced by about 50% in the presence of  $10 \text{ mM}$ - $P_i$ , indicating the final state is a mixture of  $M^* \cdot \text{ADP}$  and  $(M \cdot P_i + M \cdot \text{ADP} \cdot P_i)$  in equal concentration. It is difficult to quantify the experimental errors in  $K_{P_1}$  and  $K'_{P_1}$  determined from Figs. 6 and 9, but if the models expressed by eqn. (8) and (11) are correct then  $K_{P_1}$  ( $= 1.5 \text{ mM}$ ) falls in the range  $1.25\text{--}2.0 \text{ mM}$  and  $K'_{P_1}$  ( $= 0.5 \text{ mM}$ ) in the range  $0.25\text{--}1.0 \text{ mM}$ .

The above experiments indicate that  $P_i$  binds more weakly to  $M^* \cdot \text{ADP}$  than to  $M$  or  $M \cdot \text{ADP}$ . In view of the low signal/noise ratio of the fluorescence changes and the absence of any value for the fluorescence of  $M^* \cdot \text{ADP} \cdot P_i$  it is difficult to determine this equilibrium constant quantitatively ( $= K_5 = k_{+5}/k_{-5}$  of eqn. 7). We conclude therefore that  $K_5 > 1.5 \text{ mM}$ .

Of the possible reasons why  $P_i$  binds more weakly to  $M^* \cdot \text{ADP}$  than to  $M$ , the different conformational state of the protein seems the most likely (Bagshaw *et al.*, 1974). The existence of  $M \cdot \text{ADP} \cdot P_i$  would indicate charge repulsion of the ligands is not a significant factor. It is noteworthy in Fig. 6(b) that the ordinate intercept is zero. This indicates  $M \cdot \text{ATP} \cdot P_i$  (a complex of  $M \cdot \text{ATP}$  and  $P_i$ ) does not exist as is to be expected if the ATP and  $P_i$  binding sites on the protein are mutually exclusive. Since  $M \cdot \text{ADP} \cdot P_i$  but not  $M \cdot \text{ATP} \cdot P_i$  was detected, it is probable that  $P_i$  is binding at its catalytic site. Since the dissociation rate of  $P_i$  from  $M \cdot P_i$  is at least a 1000-fold faster than the turnover rate of the ATPase, and  $P_i$  binds more weakly to  $M^* \cdot \text{ADP}$  than  $M$ , it is probable that  $P_i$  dissociates from  $M^* \cdot \text{ADP} \cdot P_i$  very

A plot of  $(k'_{\text{obs}} - k_{+6})^{-1}$  against  $[P_i]$  at various fixed  $[\text{ADP}]$  yields a series of lines which intersect at a point with co-ordinates of  $-K_{P_1}$  (abscissa) and  $(K_{P_1} - K'_{P_1})/K'_{P_1}k_{-6}$  (ordinate). Further a plot of the gradients of these lines against  $[\text{ADP}]^{-1}$  has an intercept equal to  $1/(k_{-6}K'_{P_1})$  and a

much faster than the turnover rate, thus supporting the conclusion of Trentham *et al.* (1972). The experiments of Schenck *et al.* (1973) indicate a possible approach for measurement of the dissociation constant of  $P_i$  to  $M^* \cdot ADP$ . As  $M^* \cdot ADP \cdot P_i$  has not been characterized spectroscopically one cannot categorically rule out more general schemes for the direct breakdown of  $M^* \cdot ADP \cdot P_i$  to  $M \cdot ADP \cdot P_i$  and/or  $M^* \cdot P_i$  (an isomer of  $M \cdot P_i$ ), as well as to  $M^* \cdot ADP$  during  $Mg^{2+}$ -dependent ATPase activity. However, no results favour the general scheme and additional support for eqn. (7) being the predominant pathway is the spectroscopic and kinetic characterization of  $M^* \cdot ADP$  as an intermediate of the ATPase mechanism (Fig. 2).

Werber *et al.* (1972) reported that the amplitude of the fluorescence change of heavy meromyosin in a number of experiments was dependent on the order of addition of nucleotides and  $P_i$ . We have not repeated their experiments but have not observed such dependence in our work. We explain the larger effect of  $P_i$  on the fluorescence amplitude of ADP compared with ATP enhancement simply as a result of the weaker binding of ADP, which in turn is a reflection of the faster dissociation rate of ADP compared with the turnover rate of ATP.

Consideration of the steady-state equation (eqn. 15) of the ATPase for a system containing  $P_i$  shows that  $P_i$  competitive inhibition would be difficult to detect.

$$v = \frac{V_{\max.}}{1 + \frac{K_m}{[ATP]} \left( 1 + \frac{[P_i]}{K_{P_i}} \right)} \quad (15)$$

where  $v$  is the steady-state rate of ATP hydrolysis,  $K_{P_i} = 1.5 \text{ mM}$  and  $K_m = 10^{-7} \text{ M}$  (Lyman & Taylor, 1970). (Binding of  $P_i$  to  $M \cdot ADP$  and  $M^* \cdot ADP$  would introduce non-competitive forms of inhibition which are likely to have less inhibitory effect at  $20^\circ\text{C}$  at low  $[ADP]$  than that introduced by  $M \cdot P_i$  formation.) In the presence of  $10 \mu\text{M}$ -ATP,  $[P_i]$  would have to be  $0.15 \text{ M}$  to reduce  $v$  to  $V_{\max.}/2$  and the inhibition effect of the ionic-strength change would make characterization of the competitive inhibition difficult.

An attempt was made to determine the charge of the  $P_i$  ion binding to subfragment 1. Inhibition studies were carried out as described in Fig. 6, but in  $50 \text{ mM}$ -1,2-diaminoethane adjusted to pH 7.2 and 6.5 with HCl. The association rate of ATP itself was decreased at these pH values, but addition of  $P_i$  caused a further decrease. At pH 7.2 the dissociation equilibrium constant  $K_{P_i}$  was  $3 \text{ mM}$ . At pH 6.5 the stopped-flow traces were not monophasic and, although phosphate had an inhibitory effect with a  $K_{P_i}$  in the range  $5\text{--}15 \text{ mM}$ , the data could not be analysed according to eqn. (9). The  $pK$  of  $P_i$  at this ionic strength ( $0.16 \text{ M}$ )

is 6.8. These results indicate that  $\text{HPO}_4^{2-}$  binds competitively with respect to ATP to subfragment 1 although the complex kinetic pattern at pH 6.5 together with the uncertainty in the ionization state of proteins introduces ambiguity.

Interpretation of nucleotide binding to subfragment 1 in the presence of  $P_i$  depends on which two-step mechanism of nucleotide binding is selected. Bagshaw *et al.* (1974) have indicated why they consider eqns. (8) and (11) represent the most likely two-step binding mechanisms at ATP and ADP to the protein. The above experiments with  $P_i$  are evidence against one alternative two-step nucleotide binding mechanism [see eqn. (18) of Bagshaw *et al.*, 1974] in which an isomerization  $M$  to  $M^*$  is followed by nucleotide binding to  $M^*$ . In this mechanism binding of  $P_i$  to  $M$  and/or  $M^*$  would be expected to yield the same result insofar as dissociation constants of  $P_i$  from the protein are concerned, when the influence of  $P_i$  on the binding kinetics of either ATP or ADP was being studied. Since this was not the case, it suggests that the alternative mechanism of nucleotide binding is unlikely, although the experimental errors present in the results of Fig. 9 are such that this alternative cannot be categorically ruled out.

#### Identification of $Mg^{2+}$ -association and -dissociation steps

When the myosin steady-state complex, generated by the addition of ATP and  $Mg^{2+}$  to heavy meromyosin or subfragment 1 at  $20^\circ\text{C}$ , is treated with EDTA a loss of fluorescence enhancement is noted at a rate consistent with the turnover rate of the  $Mg^{2+}$ -dependent ATPase (Mandelkow & Mandelkow, 1973). These workers also showed that the addition of EDTA to the complex generated by the addition of ATP( $\beta,\gamma\text{-NH}$ ) to heavy meromyosin in the presence of  $Mg^{2+}$  resulted in a loss of fluorescence at a rate equal to the ATP( $\beta,\gamma\text{-NH}$ ) dissociation rate. Fig. 10 shows that, when  $M^* \cdot ADP$  is treated with excess of EDTA, the rate of the fluorescence change measured as an exponential process ( $2.1 \text{ s}^{-1}$ ) equals the rate of the ADP-dissociation process as measured by displacement techniques (Trentham *et al.*, 1972; Bagshaw *et al.*, 1972). These results suggest that  $Mg^{2+}$  dissociates very slowly from  $M^* \cdot ADP \cdot P_i$  (the predominant steady-state intermediate of the  $Mg^{2+}$ -dependent ATPase),  $M^* \cdot ATP$  [for which ATP( $\beta,\gamma\text{-NH}$ ) bound to  $M$  is an analogue] and  $M^* \cdot ADP$ . EDTA can only compete effectively for  $Mg^{2+}$  bound to unliganded nucleotides or possibly  $M \cdot ATP$  and  $M \cdot ADP$ .

Whether  $Mg^{2+}$  is bound to the nucleotide during formation of  $M \cdot ATP$  and breakdown of  $M \cdot ADP$  during the  $Mg^{2+}$ -dependent ATPase mechanism can be resolved by analysing reactions of subfragment 1 and nucleotide at various  $Mg^{2+}$  concentrations.

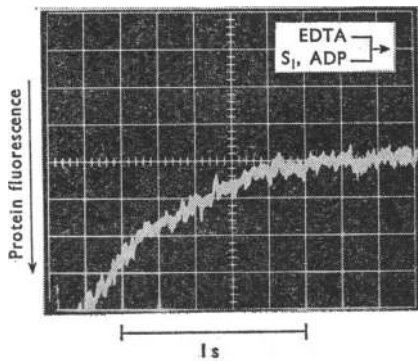


Fig. 10. Displacement of ADP from subfragment 1 by EDTA

One syringe contained 10  $\mu\text{M}$ -subfragment 1, 25  $\mu\text{M}$ -ADP and 5 mM-MgCl<sub>2</sub> and the other 20 mM-EDTA (reaction-chamber concentrations). Both syringes contained 0.10 M-KCl-50 mM-Tris adjusted to pH 8.0 with HCl.

Addition of 100  $\mu\text{M}$ -ATP to 1 mM-MgCl<sub>2</sub> gave a solution containing 9.9  $\mu\text{M}$ -free ATP and 90  $\mu\text{M}$ -MgATP in the presence of 0.1 M-KCl at pH 8.0, on the basis of a dissociation constant of Mg<sup>2+</sup> and ATP<sup>4-</sup> of  $1.00 \times 10^{-4}$  M (Martell & Schwarzenbach, 1956). Addition of 100  $\mu\text{M}$ -ATP to 5 mM-MgCl<sub>2</sub> gives a solution containing 2.0  $\mu\text{M}$ -free ATP and 98  $\mu\text{M}$ -MgATP. Increasing [MgCl<sub>2</sub>] causes [free ATP] to fall by a factor of 4.95 and [MgATP] to increase by a factor of 1.09. The rate of the fluorescence enhancement of subfragment 1 when mixed with 100  $\mu\text{M}$ -ATP was the same (within 20%, the limit of experimental accuracy) in the presence of 1 mM- or 5 mM-MgCl<sub>2</sub> in 0.1 M-KCl-50 mM-Tris adjusted to pH 8.0 with HCl. This leads to the same conclusion as Finlayson & Taylor (1969), namely that MgATP and not free ATP must be the substrate of the Mg<sup>2+</sup>-dependent ATPase, since if the latter alternative were correct, the rate of the fluorescence enhancement would decrease by a factor of 5.15 with the fivefold [MgCl<sub>2</sub>] increase. This factor includes an additional factor of 1.04 caused by the increase in ionic strength from 0.128 M to 0.140 M (Fig. 11 of Bagshaw *et al.*, 1974). Addition of 100  $\mu\text{M}$ -ADP to 1 mM- and 5 mM-MgCl<sub>2</sub> in 0.1 M-KCl at pH 8.0 gives solutions in which the [free ADP] is 45  $\mu\text{M}$  and 13.7  $\mu\text{M}$  and the [MgADP] is 55  $\mu\text{M}$  and 86  $\mu\text{M}$  respectively, on the basis of a dissociation constant of Mg<sup>2+</sup> and ADP<sup>3-</sup> of  $7.8 \times 10^{-4}$  M (Martell & Schwarzenbach, 1956). The rate of the fluorescence enhancement of subfragment 1 when mixed with 100  $\mu\text{M}$ -ADP was the same (within 30%, the limit of experimental accuracy) in the pre-

sence of 1 mM- or 5 mM-MgCl<sub>2</sub> in 0.1 M-KCl-50 mM-Tris adjusted to pH 8.0 with HCl. After correction for the change of ionic strength a decrease in rate by 3.4-fold would be expected for free ADP as ligand, and an increase in rate by 1.5-fold for MgADP as ligand. Although the small increase in association rate expected if MgADP was the ligand was not observed, it is probable that MgADP and not free ADP is the ligand for subfragment 1 because of the great similarity of the association rates of ADP and ATP to subfragment 1 in the presence of Mg<sup>2+</sup> (Bagshaw *et al.*, 1974) and the fact that MgATP is the form in which ATP binds. These results indicate that Mg<sup>2+</sup> is associated with the nucleotide at all stages of the mechanism, although it is probable that there are additional Mg<sup>2+</sup>-binding sites on myosin (Kiely & Martonosi, 1968; Mandelkow & Mandelkow, 1973).

#### H<sup>+</sup>-release experiments

When myosin or its proteolytic subfragments was mixed with excess of ATP in 0.5 M-KCl at pH 8, Finlayson & Taylor (1969) and Koretz *et al.* (1972) found there was transient H<sup>+</sup> release corresponding to about 0.5 H<sup>+</sup>/subfragment-1 site followed by steady-state H<sup>+</sup> release. They found that the rate of transient H<sup>+</sup> release is proportional to [ATP] at low [ATP], but the rate tends to reach a plateau at 200–250 s<sup>-1</sup> as the [ATP] increases. Since Bagshaw *et al.* (1974) have shown that the binding of ATP to subfragment 1 is a two-step process involving a probable isomerization of M·ATP to M\*·ATP at 200–400 s<sup>-1</sup>, it is important to establish whether the transient H<sup>+</sup> release is associated with this isomerization or with the cleavage of ATP. This can be resolved by analysing H<sup>+</sup> release of ATP analogues that bind to subfragment 1, but are not cleaved, such as ADP and ATP( $\beta,\gamma$ -NH). Since the amount of transient H<sup>+</sup> release decreased as the KCl concentration was decreased (Koretz *et al.*, 1972), stopped-flow experiments in which transient H<sup>+</sup> release was monitored by the use of pH indicators were carried out in 0.5 M-KCl. A further reason for working at 0.5 M-KCl was that the transient rate of approach to the steady state was slower in the high-salt medium, which made the observed signal easier to resolve from a small signal of unknown origin that was present (Fig. 11a). When 30  $\mu\text{M}$ -ATP was mixed with 10  $\mu\text{M}$ -subfragment 1 in the presence of Phenol Red the spectral change at 560 nm indicated transient release of  $0.37 \pm 0.3$  mol of H<sup>+</sup>/mol of subfragment 1, followed by steady-state H<sup>+</sup> release (Fig. 11b). The exponential rate of approach to the steady state was 16 s<sup>-1</sup>. When the experiment was repeated with 30  $\mu\text{M}$ -ADP or 100  $\mu\text{M}$ -ATP( $\beta,\gamma$ -NH) replacing ATP, again 0.37 mol of H<sup>+</sup>/mol of subfragment 1 was released, but at rates of 9.5 and 4.0 s<sup>-1</sup> respectively (Figs. 11c and 11d). The slower rate of H<sup>+</sup> release when 100  $\mu\text{M}$ -ATP( $\beta,\gamma$ -NH)

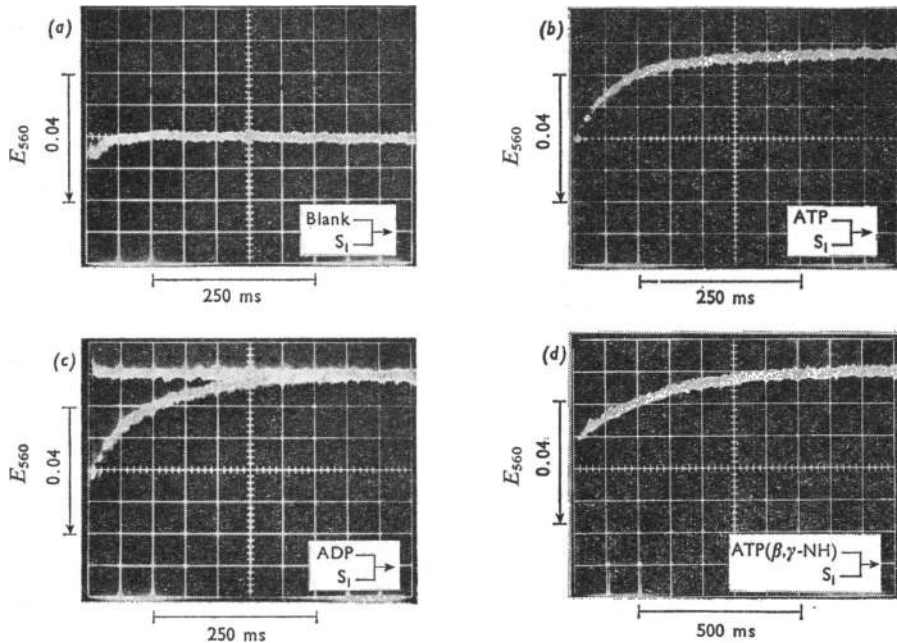
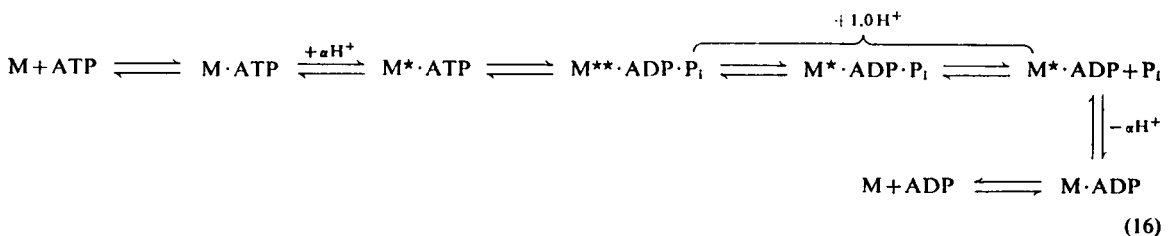


Fig. 11. Spectrophotometric records at 560nm of the reaction at 21°C between adenine nucleotides and subfragment 1 in the presence of the pH indicator Phenol Red

One syringe of the stopped-flow apparatus contained 10 μM-subfragment 1 (S<sub>1</sub>) and the other nucleotide, if present, and 25 μM-Tris. Both syringes contained 0.50M-KCl, 5mM-MgCl<sub>2</sub> and 37 μM-Phenol Red. The pH of solutions was adjusted to 8.0 as described in the Materials and Methods section. Concentrations of nucleotides were as follows: (a) zero; (b) 30 μM-ATP; (c) 30 μM-ADP; (d) 100 μM-ATP(β,γ-NH). The horizontal trace in (c) was obtained by triggering the oscilloscope a few seconds after the solutions had been mixed and indicated end-point stability. In contrast, in (b), steady-state H<sup>+</sup> release occurred so that the absorption of the solution continued to decrease after the transient phase. The spectral change in (a) occurred at a constant rate, but had an amplitude variation equivalent to between 0 and 0.11 mol of H<sup>+</sup> released/mol of subfragment 1.

was bound reflects the smaller apparent second-order association rate of ATP(β,γ-NH) relative to ATP. This result indicates that transient H<sup>+</sup> release is associated with isomerization steps rather than cleavage. Further, since the fluorescence work has established that the complex generated by mixing ADP and subfragment 1 is an intermediate of the

ATPase reaction, this experiment shows that any H<sup>+</sup> released during ATP binding is taken up when ADP dissociates. This means that an additional 1.0mol of H<sup>+</sup>/mol of subfragment 1 must be released in other steps of the ATPase mechanism, as overall 1.0mol of H<sup>+</sup> is released/mol of ATP hydrolysed at pH 8.0. These H<sup>+</sup>-release steps are identified in eqn. (16):





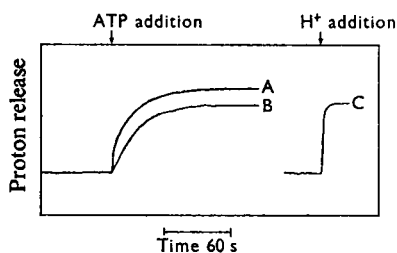


Fig. 12. Records of  $H^+$  release measured with a pH meter and glass electrode when ATP was added to subfragment 1 in the presence or absence of ADP at pH 8.0 and 21°C

In (A) 16  $\mu$ M-ATP (taken from a stock solution of ATP in the presence of  $MgCl_2$  as described in the Materials and Methods section) was added to 6ml of a stirred solution adjusted to pH 8.0 of 20  $\mu$ M-subfragment 1, 0.10M-KCl, 5mM- $MgCl_2$  and 0.12mM-Tris. In (B) 16  $\mu$ M-ATP was added to the same solution, which now contained 32  $\mu$ M-ADP (generated from ATP by action of the subfragment-1 ATPase). In (C) 16  $\mu$ M standard acetic acid was added. The pH change associated with the addition of standard acid was 0.06. Between experiments the pH was readjusted to 8.0 by addition of KOH.

The value of  $\alpha$  is 0.37 in 0.5M-KCl at pH 8. Within experimental sensitivity no  $H^+$  release could be detected in the cleavage step ( $M^* \cdot ATP \rightleftharpoons M^{**} \cdot ADP \cdot P_i$ ).

The conclusions expressed in eqn. (16) could be tested directly by measuring  $H^+$  release with a glass electrode and a pH-meter. The basis of the experiments was as follows. ATP was added to an excess of subfragment 1 and the time-course and stoichiometry of  $H^+$  release was measured. If subfragment 1 was at sufficiently high concentrations so that all ADP produced remained bound, then in terms of eqn. (16) the overall transformation would be from  $M+ATP$  to  $M^* \cdot ADP+P_i$  and  $(1.0+\alpha)$  mol of  $H^+$  should be produced/mol of ATP hydrolysed. If some ADP dissociated then between 1.0 and  $(1.0+\alpha)$  mol of  $H^+$  would be produced/mol of ATP hydrolysed. Whatever the affinity of ADP for subfragment 1 the rate profile of  $H^+$  production would be biphasic with  $\alpha$  mol of  $H^+$  produced/mol of ATP in the faster phase. In a second experiment the protein was saturated with ADP and so existed as  $M^* \cdot ADP$ . ATP was added to an excess of  $M^* \cdot ADP$  and again the time-course and stoichiometry of  $H^+$  release were measured. In terms of eqn. (16) the overall transformation would be from  $M^* \cdot ADP+ATP$  to  $M^* \cdot ADP+ADP+P_i$  and 1.0 mol of  $H^+$  should be produced/mol of ATP hydrolysed with a monophasic rate profile.

For the pH-meter experiment the overall dissociation constant of ADP to subfragment 1 must be

known. This can be evaluated kinetically, and according to eqn. (7) effectively equals  $K_6K_7$  (Bagshaw *et al.*, 1974) and is 0.95  $\mu$ M at pH 8 in 0.1M-KCl.

$H^+$  release was measured when 16  $\mu$ M-ATP was added to 20  $\mu$ M-subfragment 1 in 0.1M-KCl at pH 8. Biphasic  $H^+$  release was observed; the more rapid  $H^+$  release was limited by the electrode response time and this was followed by slow  $H^+$  release at 0.048  $s^{-1}$ , which equals the turnover rate of the ATPase (Fig. 12, trace A): 1.20 mol of  $H^+$  was released/mol of ATP added. In a second experiment 16  $\mu$ M-ATP was added to 20  $\mu$ M-subfragment 1 in the presence of 32  $\mu$ M-ADP (Fig. 12, trace B). In contrast with trace A, monophasic  $H^+$  release was observed at a rate of 0.050  $s^{-1}$ ; 1.01 mol of  $H^+$  was released/mol of ATP added. The disappearance of the rapid phase in trace B was not caused by a slow rate-limiting dissociation of ADP from the protein, since the dissociation rate is 30 times the observed rate of trace B (Fig. 6 of Bagshaw *et al.*, 1972; that experiment was repeated and found to be reproducible with the subfragment-1 preparation used in Fig. 12). Further, in the experiments described in Fig. 12 ADP was not effectively competitive with ATP, since the rates of the slow phases were not influenced by the presence of ADP. The results shown in Fig. 12 are those predicted by eqn. (16). Taking the dissociation constant of ADP from subfragment 1 as 0.95  $\mu$ M, 86% of the ADP generated in the first experiment (Fig. 12, trace A) remained bound to subfragment 1 so that  $\alpha = 0.23 (=0.20/0.86)$  in 0.1M-KCl at pH 8.

Similar experimental results to Fig. 12 were obtained from pH-meter experiments carried out in 0.5M-KCl and at pH 8 with both subfragment 1 and myosin. The experiment (Fig. 12) reinforces the conclusions of the pH-indicator experiment in a number of important ways. First, measurement of  $H^+$  release is more direct and is based on the nucleotide concentration which can be estimated with less than 1% error. Secondly, possible interaction of the dye with the protein is eliminated, although in practice no interaction of dye with subfragment 1 was detected in the control experiment described in the Materials and Methods section. Thirdly, it tests the important prediction that under certain reaction conditions more than 1 mol of  $H^+$  is produced/mol of ATP hydrolysed at pH 8. On the other hand the indicator experiment is capable of better time-resolution.

The fact that no  $H^+$  was released in the cleavage step indicates that its equilibrium constant,  $K_3$ , should be independent of  $[H^+]$ . At pH 8,  $K_3 = 9$  (Bagshaw & Trentham, 1973).  $K_3$  measured at pH 7.0 and 8.5 by the same technique was 9 and 8 respectively ( $k_{-2}$  was  $<0.02 s^{-1}$  at both pH values). This constant value of  $K_3$  over a 30-fold range of  $[H^+]$  supports the conclusions of the  $H^+$  release experiments.

Yamada *et al.* (1973) found that the enthalpy changes within a few seconds of mixing ADP and ATP with heavy meromyosin were approximately the same. From this they concluded that no  $H^+$  was released in the cleavage step. Their results were also consistent with our finding that ADP and ATP binding to protein causes the same amount of  $H^+$  release. Their conclusion that no  $H^+$  was released on nucleotide binding was an overinterpretation of their results and was based on the fact that the mixing of ADP and heavy meromyosin was considered to be a control reaction with no  $H^+$  release. However, there seems no *a priori* reason why the enthalpy changes associated with the binding and cleavage of ATP should be the same as that for ADP binding even if the concomitant  $H^+$  release is the same for both nucleotides. Further, inspection of their experimental data indicates that the enthalpy change associated with the ATP reaction during the rapid phase may be as much as 20 kJ/mol of heavy meromyosin less negative than that of the ADP reaction, though the instrument response time of 5 s makes accurate quantitative evaluation difficult.

### Conclusion

Studies on the nature of myosin-ADP complexes have led to extension of the kinetic scheme for the  $Mg^{2+}$ -dependent ATPase of myosin proposed by Lynn & Taylor (1970) and two possible schemes were presented by Seidel & Gergely (1972). The fluorescence data presented here distinguish these models and support the mechanism reported by Trentham *et al.* (1972), which requires a change in the composition of the steady-state complex under conditions where the  $M^* \cdot ADP$  dissociation rate approaches the ATPase turnover rate. This change may be brought about by the lowering of the temperature from 21°C to 5°C as suggested by Martonosi & Malik (1972), and confirmation of their proposal is provided by independent means. Extension of the scheme to eqn. (7) does not alter the fundamental arguments used here, but adds to the characterization of the nature of the  $M^* \cdot ADP$  complex. The fluorescence enhancement of subfragment 1 on binding a nucleotide is not evidence itself for a conformational change. But establishing that the process is first order at high nucleotide concentrations and occurs at a rate which depends on the type of muscle from which the myosin was prepared strongly implies the involvement of a protein-conformation change (Bagshaw *et al.*, 1974). When ADP dissociates from  $M^* \cdot ADP$  a reversal of this conformational change seems to occur, and it is this step that exhibits the marked temperature-dependence. This phenomenon itself warrants further discussion, since a 20-fold change in rate over a 15°C temperature range corresponds to an

activation energy of 300 kJ/mol. Typical values for enzyme-catalysed reactions, including the overall turnover of ATP by myosin, in the 0–30°C range are in the order of 50 kJ/mol. Large activation energies are often associated with co-operative structural transitions of macromolecules (Talsky, 1971). Further work is required on the dissociation rate and intrinsic fluorescence yield of the  $M^* \cdot ADP$  complex over a wider temperature range and by using small temperature intervals to detect if any transition points are present. A transition point has been reported in the Arrhenius plots of the steady-state rate of actomyosin ATPase (Levy *et al.*, 1962), but this may be due to changes in the aggregation state of the protein molecules, since myosin and acto-heavy meromyosin yield linear plots over the 5–30°C range (Barouch & Moos, 1971). A change in the rate-determining step of a reaction on temperature perturbation results in a non-linear Arrhenius plot (Talsky, 1971; Gutfreund, 1972, p. 165); however, such a transition is not sharp. A theoretical Arrhenius plot can be constructed from the data of Table 1, assuming that the activation energies of the steps associated with  $k_{+a}$  and  $k_{+b}$  are independent of temperature. The transition from one linear part of the Arrhenius plot to the other for the catalytic rate occurs over about 20°C and, in fact the second linear part, when  $k_{+b}$  becomes solely rate-limiting, is not attained until below –5°C. The deviation from linearity of an Arrhenius plot for the steady-state rate of the subfragment-1 ATPase should be experimentally detectable, particularly if low-temperature kinetic techniques could be applied (Hui Bon Hoa & Douzou, 1973).

$H^+$  release or uptake that occurs concomitant with the protein-conformation changes probably reflects an accumulation of small pK changes of amino acid side chains. The absence of any measurable  $H^+$  release in the cleavage step, which  $^{18}O$  experiments indicate is also the hydrolysis step (Sartorelli *et al.*, 1966; Bagshaw & Trentham, 1973), contributes to the relatively small negative  $\Delta G^\circ$  for this step. A rudimentary estimate of this contribution is –7 kJ/mol at pH 8 from the difference in free energies of hydrolysis of ATP in the presence of 5 mM- $Mg^{2+}$  at pH 8 and pH 6.2, when overall 1 and 0 mol of  $H^+$  are produced/mol of ATP hydrolysed respectively (Alberty, 1969). Boyer *et al.* (1973) have listed a number of reasons why the hydrolysis step of an ATP-protein complex is likely to be readily reversible. The absence of  $H^+$  release in this step of the myosin ATPase (and perhaps in corresponding steps of systems involving ATP synthesis) should be added to their list.

We are grateful to Professor H. Gutfreund and Dr. S. E. Halford for helpful discussions, to Dr. J. J. Holbrook for help with the fluorescence studies, and to the Science Research Council for financial support.

## References

- Alberty, R. A. (1969) *J. Biol. Chem.* **244**, 3290–3302
- Bagshaw, C. R. & Trentham, D. R. (1973) *Biochem. J.* **133**, 323–328
- Bagshaw, C. R., Eccleston, J. F., Trentham, D. R., Yates, D. W. & Goody, R. S. (1972) *Cold Spring Harbor Symp. Quant. Biol.* **37**, 127–135
- Bagshaw, C. R., Eccleston, J. F., Eckstein, F., Goody, R. S., Gutfreund, H. & Trentham, D. R. (1974) *Biochem. J.* **141**, 351–364
- Barouch, W. W. & Moos, C. (1971) *Biochim. Biophys. Acta* **234**, 183–189
- Bock, R. M., Ling, N.-S., Morell, S. A. & Lipton, S. H. (1956) *Arch. Biochem. Biophys.* **62**, 253–264
- Boyer, P. D., Cross, R. L. & Momsen, W. (1973) *Proc. Nat. Acad. Sci. U.S.A.* **70**, 2837–2839
- Finlayson, B. & Taylor, E. W. (1969) *Biochemistry* **8**, 802–810
- Godfrey, J. E. & Harrington, W. F. (1970) *Biochemistry* **9**, 894–908
- Gutfreund, H. (1972) *Enzymes: Physical Principles*, Wiley-Interscience, London, New York, Sydney and Toronto
- Harrington, W. F. & Himmelfarb, S. (1972) *Biochemistry* **11**, 2945–2952
- Holbrook, J. J. (1972) *Biochem. J.* **128**, 921–931
- Hui Bon Hoa, G. & Douzou, P. (1973) *J. Biol. Chem.* **248**, 4649–4654
- Kiely, B. & Martonosi, A. (1968) *J. Biol. Chem.* **243**, 2273–2278
- Koretz, J. F., Hunt, T. & Taylor, E. W. (1972) *Cold Spring Harbor Symp. Quant. Biol.* **37**, 179–184
- Levy, H. M., Sharon, N., Ryan, E. M. & Koshland, D. E. (1962) *Biochim. Biophys. Acta* **56**, 118–126
- Lynn, R. W. & Taylor, E. W. (1970) *Biochemistry* **9**, 2975–2983
- Mandelkow, E. & Mandelkow, E. (1973) *FEBS Lett.* **33**, 161–166
- Martell, A. E. & Schwarzenbach, G. (1956) *Helv. Chim. Acta*, **39**, 653–661
- Martonosi, A. & Malik, M. N. (1972) *Cold Spring Harbor Symp. Quant. Biol.* **37**, 184–185
- Morita, F. (1967) *J. Biol. Chem.* **242**, 4501–4506
- Rodbell, M., Birnbaumer, L., Pohl, S. L. & Krans, H. M. J. (1971) *J. Biol. Chem.* **246**, 1877–1882
- Sartorelli, L., Fromm, H. J., Benson, R. W. & Boyer, P. D. (1966) *Biochemistry* **5**, 2877–2884
- Schaub, M. C. & Watterson, J. G. (1973) *FEBS Lett.* **30**, 305–308
- Schenck, H., Mannherz, H. G. & Goody, R. S. (1973) *Hoppe-Seyler's Z. Physiol. Chem.* **354**, 234
- Seidel, J. C. & Gergely, J. (1972) *Cold Spring Harbor Symp. Quant. Biol.* **37**, 187–193
- Talsky, G. (1971) *Angew. Chem. Int. Ed. Engl.* **10**, 548–554
- Trentham, D. R., Bardsley, R. G., Eccleston, J. F. & Weeds, A. G. (1972) *Biochem. J.* **126**, 635–644
- Viniegra, G. & Morales, M. F. (1972) *J. Bioenerg.* **3**, 55–64
- Werber, M. M., Szent-Györgyi, A. G. & Fasman, G. D. (1972) *Biochemistry* **11**, 2872–2883
- Yamada, T., Shimizu, H. & Suga, H. (1973) *Biochim. Biophys. Acta* **305**, 642–653
- Yount, R. G., Babcock, D., Ballantyne, W. & Ojala, D. (1971) *Biochemistry* **10**, 2484–2489